ZINC OXIDE NANOPARTICLES MEDIATE BACTERIAL TOXICITY IN MUELLER-HINTON BROTH VIA Zn^{2+}

By

ALEXANDER J. CARON

Bachelor of Science, 2022
Texas Christian University
Fort Worth, TX

Submitted to the Graduate Faculty of the
College of Science and Engineering
Texas Christian University
in partial fulfillment of the requirements
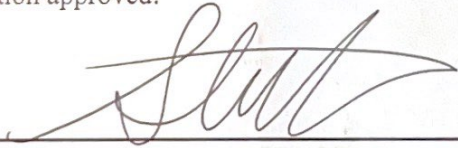for the degree of

Masters of Science

May 2024

ZINC OXIDE NANOPARTICLES MEDIATE BACTERIAL TOXICITY IN MUELLER-HINTON BROTH VIA Zn^{2+}
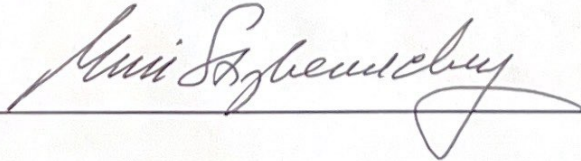
by

Alexander Jacob Caron

Dissertation approved:

_____
Major Professor

_____

_____

_____

_____
For The College of Science and Engineering

Table of Contents

Vita

Abstract

List of Figures

List of Tables

Introduction

There is an antibiotic crisis looming due to the rise of antibiotic-resistant infections coupled with decreased development of new antimicrobials (Fischbach & Walsh, 2009; Tacconelli et al., 2018). As such, there is a need for the development of novel, non-traditional antibiotics to treat antibiotic-resistant infections (Modi et al., 2022). Recent advances in nanoscale engineering have generated interest in nontraditional, inorganic antimicrobial agents such as metals and metal oxide nanoparticles (NPs) as such agents. NPs range from 1 to 100 nanometers and their small size results in a high surface-to-volume ratio which in turn impacts their physicochemical properties (Modi et al., 2022; Sirelkhatim et al., 2015) and have been shown to have broad-spectrum activity including against multi-drug resistant pathogens such as methicillin-resistant *Staphylococcus aureus* (MRSA) (Ali et al., 2021; de Lucas-Gil et al., 2019; Kadiyala, Turali-Emre, Bahng, Kotov, & Vanepps, 2018), *Escherichia coli* (Preeti et al., 2020), *Acinetobacter baumannii* (Tiwari et al., 2018), *Klebsiella pneumonia* (de Lucas-Gil et al., 2019), and *Mycobacterium tuberculosis* (Heidary et al., 2019). One such metal oxide NP that demonstrates suitable antimicrobial activity is zinc oxide nanoparticles (ZnO NPs). ZnO NPs are particularly promising due to their antibacterial activity and low cost (Gudkov et al., 2021; Lallo Da Silva et al., 2019; Sirelkhatim et al., 2015). ZnO NPs can be cheaply synthesized via multiple methods which confer highly variable chemical and physical properties which influence the antibacterial efficacy of the particles. Additionally, ZnO NPs contain properties, such as resistance to high heat and pressure and minimal production of harmful by-products, that make them amenable to applications in water purification, meat packaging, food canning, and coatings on medical implants, (Akbar et al., 2019; Q. Li et al., 2008; Sirelkhatim et al., 2015; Smaoui et al., 2023). Their long-term stability compared to traditional organic antibiotics also imparts

potential utilization in remote regions of the world that do not have access to electricity or refrigeration (Modi et al., 2022).

Despite a large body of literature showing the effectiveness of ZnO NPs, the antibacterial mechanism of ZnO NPs is still unclear. Elucidating the mechanism may allow the design of more effective ZnO NPs as altering physical properties such as size, shape, polarity, and/or surface properties can change their electrochemical and thus antimicrobial properties (Gudkov et al., 2021; Lallo Da Silva et al., 2019). There are three prevailing theories as to the mechanism of ZnO antimicrobial activity. The first is production of reactive oxygen species (ROS), and in particular hydrogen peroxide (H_2O_2) (Gudkov et al., 2021; Lallo Da Silva et al., 2019; Siddiqi, Ur Rahman, Tajuddin, & Husen, 2018; Sirelkhatim et al., 2015; Tiwari et al., 2018; X. Xu et al., 2013). The second is physical damage due to direct interactions between particles and the cell that leads to membrane disruption, loss of cytoplasmic contents, and lysis (Akbar et al., 2019; Feris et al., 2010; Gudkov et al., 2021; Joe et al., 2017; Lallo Da Silva et al., 2019; Siddiqi et al., 2018; Sirelkhatim et al., 2015). The final is release of toxic Zn^{2+} ions from the ZnO NP surface that causes mis-metalation of enzymes and disruption of ionic homeostasis (de Lucas-Gil et al., 2019; Gudkov et al., 2021; Lallo Da Silva et al., 2019; Pasquet et al., 2014; Siddiqi et al., 2018; Sirelkhatim et al., 2015; Song et al., 2020). Currently, it is unclear whether multiple of these mechanisms contribute to ZnO NP toxicity, or if there is a dominant mechanism that mediates the activity. It has been proposed that the lack of a specific molecular target, and the possibility of multiple modes of action may make it more difficult for bacteria to gain resistance to ZnO NPs, further bolstering its promise as an antibacterial agent (Lallo Da Silva et al., 2019; Slavin, Asnis, Häfeli, & Bach, 2017).

Production of ROS has been the most commonly proposed mechanism of action largely due to multiple studies that demonstrate that ZnO NPs can directly or indirectly produce ROS. Despite this, the ability to produce ROS appears highly dependent on the context and conditions of the ZnO NPs. Some data indicates light is required to activate the production of ROS; however, this is contradicted by other studies indicating light is unnecessary (Joe et al., 2017; X. Xu et al., 2013). Of all the ROS, H_2O_2 has been the predominant species proposed to mediate this action due to its ability to cross the bacterial membrane (Lallo Da Silva et al., 2019). ZnO NPs are believed to act as a catalyst surface to initiate a cascade of oxidation reactions that results in the production of H_2O_2. This cascade begins as dissolved oxygen molecules are transformed into superoxide radical anions (O_2^-). The O_2^- molecules then react with H^+ to form HO_2 which can pick up electrons and become hydroxyl peroxide anions ($HO2^-$). HO_2^- is inherently unstable and will react with H^+ to form H_2O_2 (Lallo Da Silva et al., 2019; Y. Li, Liao, & Tjong, 2020). Downstream, the H_2O_2 and other ROS can lead to double-stranded breaks in DNA that disrupt DNA replication, and lipid peroxidation that results in disruption of the bacterial membrane. Together, it has been proposed that this damage is responsible for the ZnO NP-mediated toxicity.

In addition to the production of ROS, the role of physical interactions between bacterial structures and NP surfaces has been investigated as a possible mechanism of action. It has been proposed that 1) ZnO NPs are internalized, allowing damage to intracellular structures such as DNA or proteins or 2) ZnO NPs act extracellularly to disrupt bacterial membranes and cause loss of intracellular contents. Previously, in Reeks et al., we demonstrated using ZnO microparticles too large to be internalized, that internalization is not necessary to mediate ZnO NP toxicity, however, this work was unable to make conclusions regarding the importance of disruption of

the bacterial membrane (Reeks et al., 2021). Previous work from other labs used SEM and TEM to support that physical contact induces damage and morphological changes to the bacterial envelope (Akbar et al., 2019; Dhanasegaran et al., 2022; Y. Liu et al., 2009; Manzoor et al., 2016). Although some groups have attempted to identify some of the specific functional groups that ZnO interacts with, it is unknown whether electrostatic interactions between negatively charged bacterial membranes and polar surfaces on the ZnO NPs mediate these interactions. Though many sources report contact with ZnO NPs, few of them have evaluated ZnO cytotoxicity in the absence of physical contact. As a result, it is possible that damage to the cell membrane may occur through a mechanism independent of physical contact or that there are additional methods outside of physical interactions that mediate ZnO toxicity.

Lastly, dissolution of toxic Zn^{2+} ions has also been proposed as a potential mechanism (Gudkov et al., 2021; Sharma, Shukla, Sharma, & Kumar, 2022; Siddiqi et al., 2018; Sirelkhatim et al., 2015; Slavin et al., 2017). Zn^{2+} toxicity may occur through two mechanisms: 1) mis-metalation of enzymes that require metal cofactors leading to protein dysfunction and 2) disruption of osmotic homeostasis. While the exact role of Zn^{2+} in cytotoxicity is still unconfirmed, the ability of Zn^{2+} ions to induce bacterial death has been established. The majority of evidence supporting release of toxic Zn^{2+} as the mechanism comes from studies investigating the relationship between the ZnO NP surface and interactions with the media (Johnson et al., 2022; M. Li, Zhu, & Lin, 2011) however, this activity seems to be highly dependent on the type of media and ZnO NPs used.

Although antibiotics can and have been used in the absence of understanding the mechanisms that mediate their toxicity, elucidating the mechanism of action of ZnO NPs is especially important as the NPs could be engineered to have increased antibacterial activity. If

we understand the properties that confer the antimicrobial activity, then it may be possible to modify the properties of the ZnO NPs via alterations in synthesis methods to increase the antibacterial efficacy. As such the purpose of this study was to investigate which of the three previously discussed mechanisms of action mediate ZnO activity. We chose to investigate ZnO NP-mediated bacterial toxicity using *S. aureus* due to its clinical relevance and previous work showing its susceptibility, including MRSA strains, to ZnO NPs (Ali et al., 2021; de Lucas-Gil et al., 2019; Kadiyala et al., 2018). In addition to being one of the major causes of skin and soft tissue infections in the US (DeLeo & Chambers, 2009), MRSA is classified as a "serious threat" by the CDC and a high-priority pathogen by the WHO ("Antibiotic resistance threats in the United States, 2019," 2019). The virulence of *S. aureus* has also been well-studied and many genetic mutants exist that can be used to test resistance mechanisms (Cheung, Bae, & Otto, 2021). We sought to accomplish this using wild-type and mutant *S. aureus* to investigate the importance of media type, hydrogen peroxide (H_2O_2), physical contact, and cell charge for the antimicrobial properties of zinc oxide. Additionally, we evaluated the ability of *S. aureus* to become resistant to ZnO NPs and sought to identify the genetic properties that conferred this resistance as an additional method of identifying the antimicrobial mechanism of ZnO. Better insight into the antimicrobial mechanism of ZnO NP will allow researchers to develop morphologies that are optimized for microbial cytotoxicity. Development of more efficacious particles could lead to widespread implementation of ZnO as a sterilization tool in food handling/packaging and the medical field.

Materials and Methods

Bacterial strains and reagents

S. aureus strains (Newman or SA113) were grown in MHB (Hardy Diagnostics) at 37°C under aerobic (shaking) conditions unless otherwise noted. *S. aureus* Δ*katA* and Δ*mprF*, were created previously (Park, Nizet, & Liu, 2008; Peschel et al., 2001) with Δ*katA* from the Newman parental strain and Δ*mprF* from SA113. ZnO NPs were acquired from Sigma-Aldrich, Zochem, or Alfa Aesar. All other antimicrobials (H_2O_2, daptomycin, $ZnCl_2$, and $MgCl_2$) were purchased from Sigma-Aldrich.

ZnO Morphology Characterization

Scanning Electron Microscopy (SEM) was used to characterize the morphology of nanoparticles. This was done using a JEOL field emission scanning electron microscope. The samples were mounted inside the SEM chamber and observed under a 15 kV electron beam for morphology characterization.

MIC assays

Cultures were grown to an optical density (OD) of 0.4 at 600nm and then diluted 1:200 to approximately $1x10^6$ cfu/ml for all assays. For ZnO NP assays, bacteria were added to microcentrifuge tubes with the indicated concentrations of ZnO NPs in a final volume of 400 μl. The microcentrifuge tubes were continuously inverted for 16-20 hours at 37° C to maximize interactions between ZnO NPs and *S. aureus*. Microcentrifuge tubes containing the same concentrations of ZnO NPs in 400 μl MHB without *S. aureus* were co-incubated at the same time. After incubation, the microcentrifuge tubes were centrifuged at 100 rpm for 2 minutes to separate the ZnO NPs from the *S. aureus*. 200 μl of supernatant was then transferred into a 96-well plate and the OD_{600} values were measured using a Fluostar Omega plate reader (BMG Labtech). The background turbidity from residual ZnO NPs was removed by subtracting the

OD_{600} readings for the ZnO control tubes from the tubes containing *S. aureus* and the same concentration of ZnO NPs. For MIC assays using H_2O_2, daptomycin, $ZnCl_2$, or $MgCl_2$, the assays were performed in 96-well plates in a final volume of 200 μl and incubated under static conditions for 16-20 hours. For daptomycin assays, MHB was supplemented with 50 μg/ml $CaCl_2$. To control for background turbidity caused by the salts ($MgCl_2$ and $ZnCl_2$), the OD_{600} of wells with the same concentration of salt without *S. aureus* were subtracted from the OD_{600} readings from the wells containing the same concentration of salt with *S. aureus.* All MIC assays were performed a minimum of three times.

Generation of Resistance

In initial attempts to generate resistance, *S. aureus* (Newman) was grown in a sublethal concentration of 0.313 mg/ml of ZnO (Sigma Aldrich) for 24 hours and passed daily into fresh ZnO-containing media by centrifuging at 200 rcf for 30 seconds to pellet the ZnO and transferring 20 μl of supernatant into a new 1.75 ml microcentrifuge tube. Additionally, a tube of *S. aureus* was passed in the absence of ZnO as a parental control to account for natural variation due to the accumulation of stochastic mutations. Minimum inhibitory concentration (MIC) assays were conducted on days 0, 2, 4, 6, 8, 10, and 15 by inoculating 3 ml of MHB with 35 μl of the passaged *S. aureus*, growing to an OD_{600} of 0.4, and then further diluting to a final ratio 1:200 in MHB before conducting ZnO MIC assays as described below. Data are plotted as fold change from the original log phase MIC of 1.25 mg/ml. After freezing down and restreaking these intermediately ZnO-resistant cultures, a second attempt to generate resistance was made in which the same protocol was followed except the sublethal dose that cultures were passed at was increased as a change in MIC was observed. During the second attempt, MICs were conducted every 5 days to measure the change in resistance.

DNA Extraction and Whole Genome Sequencing (WGS)

DNA extractions were performed using the Maxwell® 16 Cell DNA Purification Kit in conjunction with the Maxwell® 16 Instrument for three ZnO^R mutants and the parental strain. Microbial whole genome sequencing was performed by Novogene. Sequencing was performed by first fragmenting genomic DNA into 350 bp fragments selected for sample purification beads. The selected fragments are then end polished, A-tailed, and ligated with the full-length adapter. Illumina PE150 technology was then employed to sequence the sample.

Identification of SNPs

Upon WGS, the bp location of all SNPs and indels was provided by Novogene. The location of the SNPs was cross-referenced against the NC_007795.1 *Staphylococcus aureus subsp. aureus* NCTC 8325 complete genome to identify what genes the SNPs are located in. SNPs were classified as in genes or between genes. Only SNPs within genes were further investigated due to a lack of functional information about inter-gene SNPs. Once SNPs were identified, they were classified as synonymous (dN) or nonsynonymous (dS) and the dN/dS ratio was calculated for each of the strains.

Gene Ontology Terms

To investigate whether any of the identified genes had conserved functions or pathways Gene Ontology (GO) terms were determined for the entire NC_007795.1 *Staphylococcus aureus subsp. aureus* NCTC 8325 chromosome, complete genome using BLAST2GO. These GO terms were applied to all the genes that contained SNPs. After applying GO terms, genes with SNPs that were encoded in the *S. aureus* genome were prioritized over prophage-encoded genes.

dUTPase BLAST

The NC_007795.1 *Staphylococcus aureus subsp. aureus* NCTC 8325 chromosome, complete genome was nBLASTed against the CP002388.1:c1489192-1488665 *Staphylococcus*

aureus subsp. aureus dUTPase to determine the location of dUTPase and the SNPs within it in our mutant strains.

Growth in ZnO NP conditioned media

Conditioned media was made by incubating 20 mg/ml of either Sigma-Aldrich or Zochem ZnO NPs in either sterile MHB, PBS, or saline in clear conical tubes at room temperature. At indicated times, the media was mixed to resuspend the ZnO NPs and a 1 ml aliquot of the media was removed and centrifuged at 16,000 rcf for 5 minutes to pellet the ZnO NPs. 100 µl of the supernatant from this aliquot was then added to an individual well of a 96-well plate. Log phase *S. aureus* was then diluted 1:100 in unconditioned MHB and 100 µl was added to the same wells for a final concentration of 50% conditioned media and approximately $1x10^6$ cfu/ml *S. aureus* in a total volume of 200 µl. As a positive control, *S. aureus* was also grown in unconditioned MHB and as a negative control, 200 µl of conditioned media (no *S. aureus*) was placed in another well. The plate was incubated under static conditions at 37° C and OD_{600} values were measured after 16-20 hours. To generate a dose curve of conditioned media, log phase *S. aureus* was diluted 1:100 and 100 µl was added to each well. Then 100 µl of media containing different ratios of conditioned:unconditioned media was added for a total volume of 200 µl containing approximately $1x10^6$ cfu/ml *S. aureus* in a final concentration of 50%, 25%, and 12.5% conditioned media. Plates were then incubated under static conditions at 37°C for 16-20 hours before reading the OD_{600} values.

Chelated media was made by adding 30 mg/ml of Chelex beads (Sigma Aldrich) to the media (either unconditioned MHB or conditioned MHB) and inverting continuously for one hour at room temperature. The mixture was then sterile filtered to remove the beads and the process was repeated. Cultures were grown to early log phase to an optical density (OD) of 0.4 at 600nm and separated into four aliquots. Each of these aliquoted cultures were pelleted and washed in

PBS two times before being resuspended in the equivalent volume of either MHB, conditioned media, chelated media, or chelated conditioned media. These aliquots were then diluted 1:50 in their respective media (MHB, chelated MBH, conditioned MHB or chelated conditioned media). 50 µl of the 1:50 cultures was then added to a 96-well plate containing 150 µl of the matching media type to produce a 1:200 final dilution (approximately 1×10^6 cfu/ml) of *S. aureus* in 100% of each media type (first 4 bars of figure 4) To produce a mix of 25% regular MHB and 75% of each media type (chelated MHB, conditioned MHB or chelated conditioned MHB), 50 µl of the *S. aureus* culture diluted 1:50 in MHB was added to a 96-well plate containing 150 µl of either chelated media, conditioned media, or chelated conditioned media. The 96-well plate was incubated under static conditions at 37° C and OD_{600} values were measured after 16-20 hours.

The concentration of Zn^{2+} in conditioned media was measured by ICP-MS at the University of Texas at Dallas Chemistry Core Facility. MHB was conditioned with 20 mg/ml ZnO NPs for either one-day or at least one-month. This conditioned media was then chelated as described above. 100 µl of each sample was diluted with 4900 µl of blank for analysis and a 50x correction factor was applied to the data. Two independent samples were measured for each condition and reported as mean ± standard deviation.

Contact-independent ZnO assays (dialysis button)

Empty dialysis buttons (Hampton Research), elastic bands, and 3.5 MWCO semipermeable dialysis tubing (ThermoFisher) were sterilized by UV radiation (254 nm) for at least 15 minutes on all sides prior to assay setup. Either 0 mg or 30 mg of ZnO NPs was loaded into sterilized dialysis buttons and sterile MHB was added until the button was completely filled. The dialysis button was then sealed with dialysis tubing soaked in sterile water and secured with elastic bands. Excess tubing was cut to size with disinfected scissors. Log phase *S. aureus* Newman (approximately 2×10^6 cfu/ml) was grown in the presence of an empty dialysis button,

30 mg free ZnO (no button), or 30 mg of ZnO inside a dialysis button in a total volume of 1.5 ml

MHB. To ensure proper sterilization of the dialysis buttons and aseptic technique, an empty

dialysis button was incubated in MHB in the absence of bacteria and served as the negative

control. To control for background turbidity of free ZnO NPs, 30 mg of ZnO NPs (no button)

was incubated in the absence of *S. aureus* in 1.5 ml of MHB. The assays were conducted in

individual wells of a 24-well tissue culture plate that was incubated at 37°C shaking at 200 rpm

for 16-20 hrs. After 16-20 hours, OD_{600} values were measured. To minimize background from

residual ZnO particles, the OD_{600} of free ZnO NPs incubated in the absence of *S. aureus* was

subtracted from the OD_{600} of free ZnO NPs incubated with *S. aureus.*

Survival Assay

S. aureus was grown to early log phase (OD600 of 0.4) in MHB, washed, and

resuspended in MHB, saline, or PBS and then diluted 1:100 in the respective medias. Diluted *S.*

aureus cultures were incubated at a 1:1 ratio with 5 mg/ml of ZnO suspended in the same media-

type for a final concentration of 2.5 mg/ml ZnO and 1:200 dilution of log-phase *S. aureus* in 1.5

ml. Tubes were mixed by inverting at 37 °C and 200 µl of culture from each tube was removed at

the indicated time points, centrifuged at 100 rcf for 2 min to pellet the ZnO particles, and serial

dilutions of the supernatant were plated to enumerate surviving cfu/ml.

Results

Commercially availiable ZnO NPs demonstrate antibacterial ability

Several previous studies have demonstrated the antimicrobial activity of ZnO NPs against

S. aureus using a variety of ZnO NP sources and assay conditions (Ali et al., 2021; Dadi,

Azouani, Traore, Mielcarek, & Kanaev, 2019; de Lucas-Gil et al., 2019; Kadiyala et al., 2018;

Raghupathi, Koodali, & Manna, 2011). One challenge in assaying the antimicrobial ability of

ZnO NPs is that they have low solubility and do not stay suspended in solution. If added to the well of a plate, particularly under static conditions, they will accumulate at the bottom, potentially creating unequal interactions between the ZnO NPs and bacteria in the well. In order to address this, we maximized interactions between the ZnO NPs and *S. aureus* by incubating them together in microcentrifuge tubes under constant inversion at 37°C. This resulted in consistent and effective inhibition of bacterial growth at an MIC of 1.25 mg/ml (15.4 mM) for ZnO NP obtained from Sigma-Aldrich (Fig. 1).

Sigma-Aldrich ZnO NPs (mg/ml)
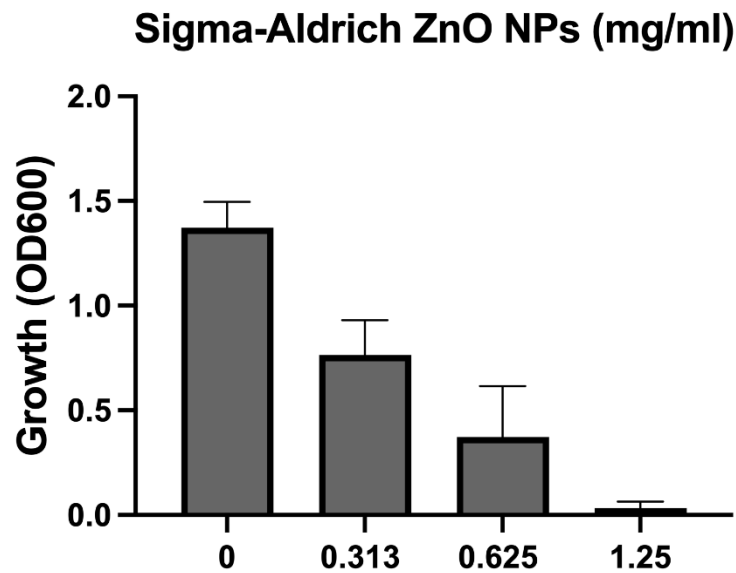
Figure 1. ZnO NPs demonstrate antibacterial action. *S. aureus* growth in Sigma-Aldrich ZnO NPs. Error bars represent +/- SD of three independent trials.

After establishing this procedure for testing the antibacterial ability of ZnO NPs, we sought to evaluate the antimicrobial ability of ZnO NPs from other commercial sources (Alfa Aesar and Zochem). We found that Alfa Aesar ZnO NPs achieved the same level of antibacterial activity with an MIC of 1.25 mg/ml, but that Zochem NPs were slightly less effective with a MIC of 2.5 mg/ml (Table 1). Because the Sigma-Alrich NPs and Alfa Aesar NPs display similar MICs as well as similar morphologies, surface areas, sizes, and purities (Table 1) we chose to

proceed with Sigma-Aldrich NPs as our primary NP for future analysis. In addition to having a

higher MIC, the Zochem NPs have a different morphology, smaller surface area, and are more

pure than the Sigma-Aldrich and Zochem NPs. Because the Zochem NPs display different

characteristics, we proceeded to use Zochem NPs in some of our subsequent analyses in order to

determine whether the properties displayed by Sigma-Aldrich NPs are specific to their particle

type or if it is more broadly applicable to general ZnO NPs.

Table 1. Comparison of commercially available ZnO sources

Particle Type	Particle Size (nm)	Morphology	Surface Area (m^2/g)	Purity	MIC (mg/ml)
Sigma Aldrich	50	granular/mixed	16	99%	1.25
Alfa Aesar	50	granular/mixed	16	99%	1.25
Zochem	280	rod-like/mixed	2-8.5	99.9%	2.5

S. aureus only gain intermediate resistance to ZnO NPs

Previous studies have suggested that ZnO toxicity occurs through multiple mechanisms

and therefore it would be difficult for bacteria to gain resistance to ZnO NPs (Lallo Da Silva et

al., 2019; Slavin et al., 2017). To investigate whether *S. aureus* can gain resistance to ZnO, we

passed *S. aureus* in triplicate in sublethal concentrations of 0.313 mg/ml ZnO and then tested

whether the MIC changed over time. We found that within one week, a two-fold increase in the

MIC was observed when *S. aureus* was passed under sublethal concentrations of Sigma-Aldrich

NPs (Fig. 2A). After another three days, a fourfold increase, as compared to day zero, was

observed, indicating that *S. aureus* rapidly gains resistance to ZnO NPs. Immediately following

the 15 days of passing, each of the ZnO resistant strains (hereby referred to as ZnO^R as a

collective, or ZnO^{R}A/B/C for individual replicates) were streaked out on a plate and aliquots

were frozen. A MIC assay was performed on each of the ZnO^R strains that had been passed

independently of each other and the ODs were averaged to confirm the resistance. In initial

attempts to quantify the resistance, we found an eight-fold change in resistance between the parental (MIC of 1.25 mg/ml) and the ZnOR strains (MIC of 10 mg/ml) (Figure 2B). In addition to culturing the ZnO^R strains on a plate at the conclusion of sublethal passing, we also froze each of the strains at -80 ^{o}C for future analysis. Unfortunately, upon re-culturing the frozen stocks several months later, we were unable to replicate the change in resistance using Sigma-Aldrich NPs (Fig. 2C) and saw only an intermediate resistance to Zochem NPs (Fig. 2D).
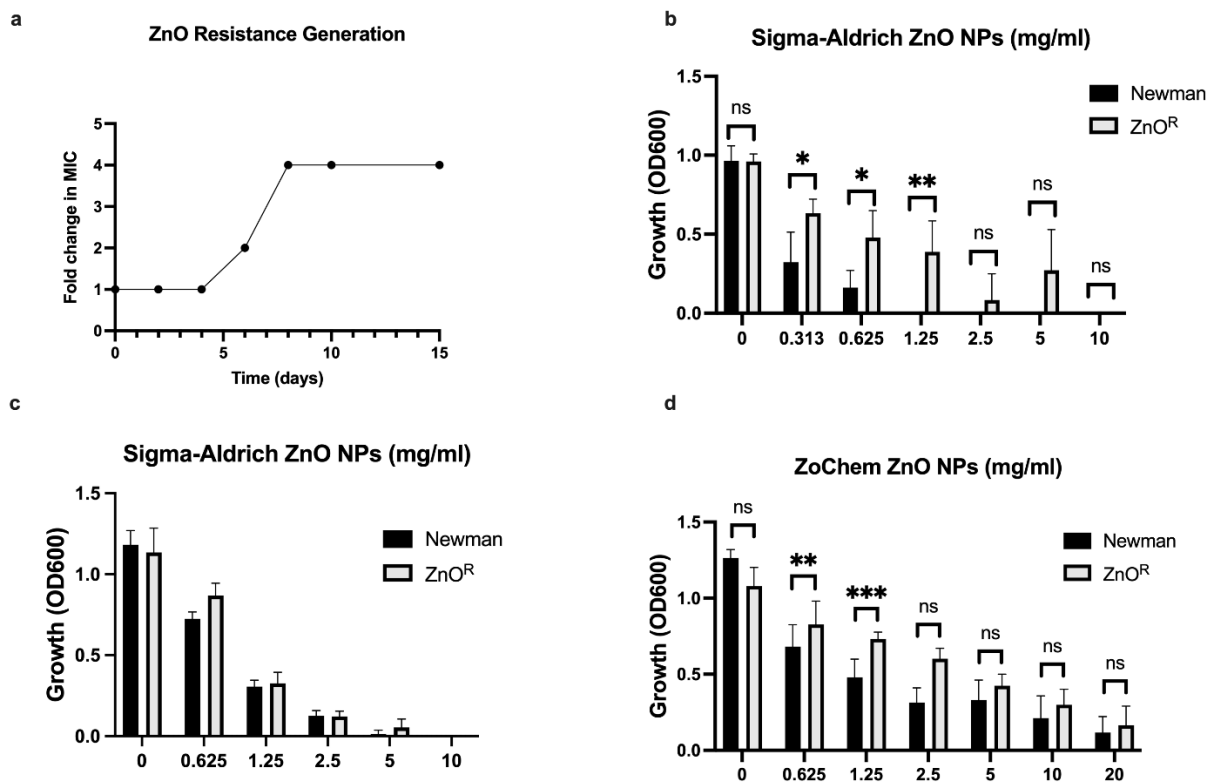
Figure 2. *S. aureus* acquired unstable, intermediate resistance to ZnO NPs. a) Fold change in MIC using Sigma Aldrich ZnO NPs over time. Growth of parental and ZnO^R *S. aureus* in b) Sigma-Aldrich ZnO NPs immediately after 15 days of resistance generation, c) Sigma-Aldrich ZnO NPs after ZnO^R strains were frozen down and restreaked d) Zochem ZnO NPs after ZnO^R strains were frozen down and restreaked. b-c) ZnO^{R}ABC strains were averaged together d) ZnO^R strains susceptibility evaluated independently. b-d) Data are presented as mean +/- SD of at least three independent trials. Statistical significance determined by unpaired t-test; *p<0.05, **p<0.01, ***p<0.001 or non-significant (ns) from parental levels within each treatment group.

One of the goals, if resistance was gained to ZnO NPs, was to characterize the genetic properties that confer the resistance as an additional route to understanding the antibacterial mechanism of ZnO NPs. Prior to testing the frozen down strains, the intermediately resistant strains were subjected to whole genome sequencing (WGS) to determine the mutations they acquired over the course of sublethal ZnO NP passing. To determine whether mutations accumulated stochastically while the ZnO^R strains were being passed or whether they were due to selection, the dN/dS ratios were independently determined for each mutant (Table 2). Each mutant had a dN/dS ratio of approximately 2.0 or higher indicating a higher number of non-synonymous mutations, and that selection may have occurred on the strains. However, the parental strain that was passed in the absence of ZnO contained a similar dN/dS ratio as compared to the ZnO^R mutants (Table 2), indicating that even in the absence of ZnO it may have

Table 2. Selection has occurred on all passed *S. aureus* strains

Strain	Synonymous	Non-synonymous	dN/dS ratio
Parental	27	61	2.26
ZnO^{R}A	27	62	2.30
ZnO^{R}B	23	61	2.65
ZnO^{R}C	35	69	1.97

experienced some selective pressure. From the WGS, we identified that 340 SNPs were conserved between the three ZnO^R mutants and were not found in the parental strain. 62 (18%) of these SNPs occurred between genes, while the other 278 (72%) occurred across 41 different genes (Table 3). In order to identify a conserved mechanism or target associated with each of the mutated genes, gene ontology analysis was performed. We discovered that 31 of the 41 genes that the SNPs were in pro-phage associated genes rather than the *S. aureus* genome itself (Table 3). Of the ten genes that were not located in phage-associated genes, only seven had published gene codes and functions (Table 4).

Table 3. Most ZnO^R-associated SNPs occur in phage-associated genes

62 SNPs (~18%) occurred between genes
278 SNPs (~72%) were distributed across 41 genes
340 SNPs total

31 Phage-Assosiated Genes
10 Non-phage Assosiated Genes
41 Total Genes

Table 4. Non-phage SNP Containing Genes

Gene code	Function
rpoC	DNA-directed RNA polymerase subunit beta
rpsL	30S ribosomal protein S12
----	helix-turn-helix domain-containing protein
----	hypothetical
hsdM2	type I restriction-modification system subunit :
dut	dUTP pyrophosphatase
scn	staphylococcal complement inhibitor SCIN
chp	chemotaxis-inhibiting protein CHIPS
sak	staphylokinase
----	DUF443 domain-containing protein

In the absence of any key genes associated with proposed mechanisms such as oxidative stress genes or cation transporters, GO term analysis was used to investigate the function and pathways associated with the 10 non-phage-associated genes because they are more likely to confer a phenotypic difference that resulted in the development of resistance. We found divalent cation binding ability, specifically Zn^{2+} ion binding, was conserved across many of these genes (Table 5). This divalent cation binding ability was especially concentrated in genes associated with DNA binding.

Table 5. Gene Ontology terms associated with the 10 *S. aureus* encoded genes containing ZnO^R-associated SNPs

Gene code	Biological Process	Molecular Function	Cellular Component
rpoC	DNA-templated transcription	DNA binding; DNA-directed 5'-3' RNA polymerase activity; zinc ion binding	DNA-directed RNA polymerase complex
rpsL	translation	tRNA binding; structural constituent of ribosome; rRNA binding	small ribosomal subunit
helix-turn-helix domain containing protein	----	DNA binding	----
Hypothetical Protein	histidine biosynthetic process; amino acid biosynthetic process; branched-chain amino acid biosynthetic process; leucine biosynthetic process; DNA restriction-modification system; primary metabolic process; small molecule metabolic process; transmembrane transport; organonitrogen compound metabolic process	DNA binding; catalytic activity; 2-isopropylmalate synthase activity; acetyl-CoA C-acetyltransferase activity; histidinol dehydrogenase activity; GTP binding; zinc ion binding; oxidoreductase activity; oxidoreductase activity, acting on the CH-OH group of donors, NAD or NADP as acceptor; transferase activity; manganese ion binding; metal ion binding; NAD binding; ABC-type transporter activity	cytoplasm; cytosol; membrane
hsdM2	DNA restriction-modification system; DNA methylation on adenine	DNA binding; N-methyltransferase activity; site-specific DNA-methyltransferase (adenine-specific) activity	Site-specific DNA-methyltransferase (adenine-specific)

dut	dUMP biosynthetic process; dUTP catabolic process	magnesium ion binding; dUTP diphosphatase activity	dUTP diphosphatase; Nucleotide diphosphatase
scn	----	----	extracellular region
chp	----	----	extracellular region
sak	plasminogen activation	----	extracellular region
DUF443 domain-containing protein	----	----	membrane

One interesting candidate that stood out in the list of nonphage-associated genes was the *dut* gene which encodes dUTPase. dUTPase catalyzes the breakdown of dUTP to dUMP, which is important in limiting the incorporation of dUMP into DNA (Kerepesi et al., 2016). Although the published function of dUTPase has no obvious ties to ZnO resistance, Kadiyala et al.) reported that *dut* and other genes responsible for UMP regulation and biosynthesis are downregulated in response to ZnO NPs (Kadiyala et al., 2018). As such, we chose to identify where in the dUTPase gene the SNPs occurred by aligning the dUTPase gene to the *S. aureus* genome to better understand if they result in loss of function or changes in expression. We found that of the 11 SNPs that were present in the dUTPase gene, 9 were present in the gene body, and 2 were present in an indel region on the interior of the gene body, suggesting that the mutations alter the functionality, rather than the

Table 6. dUTPase SNPs are in the gene body

SNP Postion (bp)	Location in DUTPase
1,952,112	Gene body
1,952,132	Gene body
1,952,185	Gene body
1,952,189	Gene body
1,952,201	Gene body
1,952,206	INDEL Region
1,952,216	INDEL Region
1,952,318	Gene body
1,952,348	Gene body
1,952,381	Gene body
1,952,417	Gene body

expression, of the dUTPase gene (Table 6). Although these mutations tentatively suggest a role of disruption of Zn^{2+} ion homeostasis and UTP regulation, the results are tempered by our later findings that the strains only gained an intermediate resistance. To strengthen these claims, we

attempted to bolster the resistance of the three previously passed ZnO^R strains by a second round of passing them at sublethal concentrations of ZnO. To improve on previous experimental design and attempt to generate a higher, more stable resistance, we increased the concentration of ZnO NPs as we passed the strains and saw increases in MIC (Fig. 3A). In this way, we could maintain a consistent sublethal concentration of (fraction of MIC) even as the MIC increased. Like the first passing, we saw that the three strains all gained a 4-fold change in MIC as compared to the parental strain (Fig. 3A).
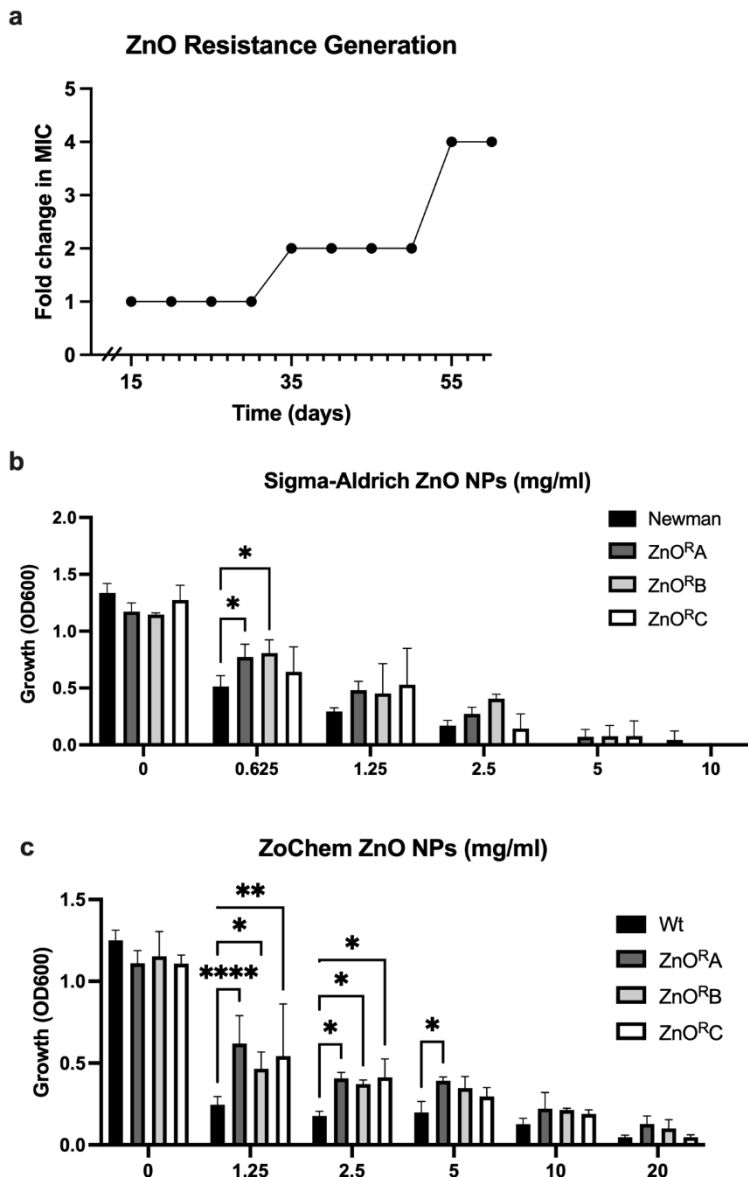
Figure 3. Additional passage of ZnO^R strains maintained intermediate phenotype a) Fold change in MIC using Sigma-Aldrich NPs over time. Growth of parental and ZnO^R *S. aureus* in b) Sigma-Aldrich ZnO NPs and c) Zochem ZnO NPs, b-c) Data are presented as mean +/- SD of at least three independent trials. Statistical significance was determined by a 2-way ANOVA followed by a Dunnett's *post hoc* test; *p<0.05, **p<0.01, ***p<0.001, ****p<0.0001, or non-significant (ns) from parental levels within each treatment group.

Despite this, when the ZnO^R strains were streaked out on plates, grown to log phase, and MIC reassessed, we saw a reversion to intermediate resistance with both Sigma-Aldrich and Zochem NPs (Fig 3B and 3C). The inability of *S. aureus* to generate stable resistance may suggest that ZnO toxicity occurs via a non-specific target or multiple independent mechanisms. In the absence of a ZnO^R mutant, we turned to using *S. aureus* strains with targeted mutations to investigate which of the previously proposed mechanisms contribute to ZnO toxicity.

Neither production of H$_2$O$_2$ nor electrostatic interactions are responsible for ZnO NP-mediated toxicity

Production of H$_2$O$_2$ by ZnO NPs has historically been the predominant theory proposed for the antibacterial properties of ZnO (Gudkov et al., 2021; Lallo Da Silva et al., 2019; Siddiqi et al., 2018; Sirelkhatim et al., 2015; Tiwari et al., 2018; X. Xu et al., 2013). The NP surface acts as a catalyst to initiate a cascade of oxidation reactions that results in the production of H$_2$O$_2$. This cascade begins as dissolved oxygen molecules are transformed into superoxide radical anions (O$_2^-$). The O$_2^-$ molecules then react with H$^+$ to form HO$_2$ which can pick up electrons and become hydroxyl peroxide anions (HO$_2^-$). HO$_2^-$ is inherently unstable and will react with H$^+$ to form H$_2$O$_2$ (Lallo Da Silva et al., 2019; Y. Li et al., 2020). In addition to being more stable than the intermediates, H$_2$O$_2$ is also neutrally charged and can diffuse through the bacterial membrane to cause intercellular damage (Lallo Da Silva et al., 2019; Y. Li et al., 2020). To evaluate the role of H$_2$O$_2$ in ZnO NP toxicity, we used a strain of *S. aureus* where the catalase gene (*katA*) was removed via allelic replacement to generate Δ*katA* (Park et al., 2008). Catalase is responsible for breaking down H$_2$O$_2$ into H$_2$O and O$_2$ and loss of the gene results in increased susceptibility to H$_2$O$_2$ (Park et al., 2008). We hypothesized that if H$_2$O$_2$ is responsible for ZnO-mediated growth inhibition, then Δ*katA* should be more susceptible to ZnO NPs than its parental strain (Newman).

a

H₂O₂ (%)

b

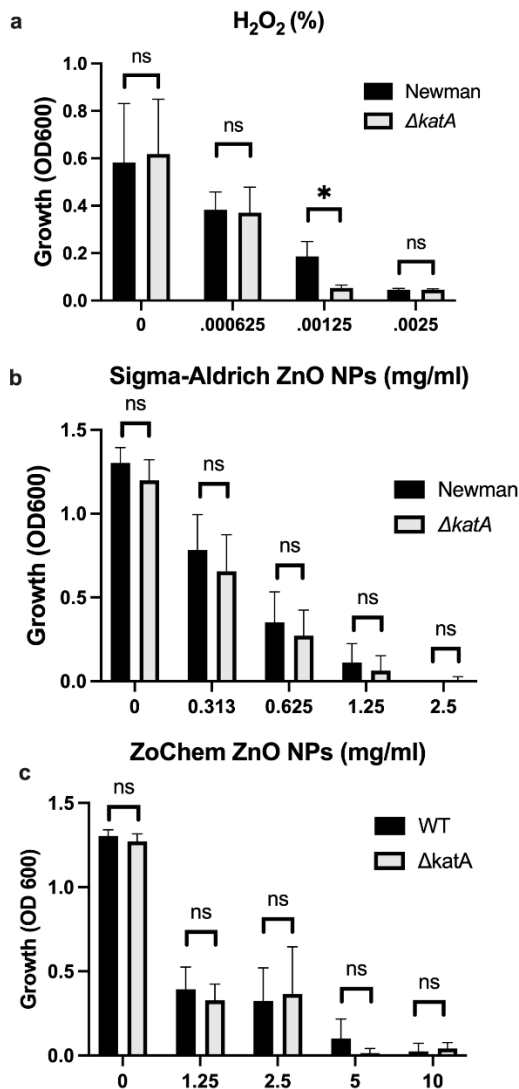**Sigma-Aldrich ZnO NPs (mg/ml)**

c

ZoChem ZnO NPs (mg/ml)

Figure 4. Production of H₂O₂ is not responsible for the antimicrobial activity of ZnO NPs. Parental (Newman) and ΔkatA *S. aureus* growth in a) H₂O₂, b) Sigma-Aldrich ZnO, and c) Zochem ZnO NPs. Data are presented as mean +/- SD of at least three independent trials. Statistical significance determined by unpaired t-test; *,p<0.05 or non-significant (ns) from parental levels within each treatment group.

We confirmed that Δ*katA* had increased susceptibility to H₂O₂ (Figure 4A), but we saw no difference in ZnO NP susceptibility (Sigma-Aldrich and Zochem) as compared to the parental strain (Figure 4B and 4C) indicating that H₂O₂ is not responsible for ZnO-mediated toxicity. Physical contact that disrupts cellular integrity is another commonly proposed mechanism of ZnO NP toxicity. Previous studies have seen evidence of physical interactions between ZnO NPs and the bacterial cell surface and reported damage to the bacterial cell membrane after exposure to ZnO NPs (Akbar et al., 2019; Feris et al., 2010; Gudkov et al., 2021; Joe et al., 2017; Lallo Da Silva et al., 2019; Siddiqi et al., 2018; Sirelkhatim et al., 2015).

Additionally, several studies have specifically implicated electrostatic interactions in mediating this contact (Arakha, Saleem, Mallick, & Jha, 2015; Feris et al., 2010). To investigate the role of electrostatic interactions in *S. aureus*, we used a *mprF* deficient strain of *S. aureus* (Δ*mprF*) (Peschel et al., 2001). MprF is responsible for synthesizing and translocating lysyl-

phosphatidylglycerol, a positively charged phospholipid, to the cell membrane. Loss of *mprF*

results in a cell envelope that is more negatively charged compared to the parental strain

resulting in increased susceptibility to cationic antimicrobial peptides such as defensins and the

antibiotic daptomycin (Ernst et al., 2009; Peschel et al., 2001). We hypothesized that if

electrostatic interactions on the bacterial envelope mediate the antibacterial activity of ZnO NPs,

ΔmprF would exhibit increased susceptibility to ZnO NPs compared to the SA113 parental

strain. We confirmed that *ΔmprF* showed increased susceptibility to daptomycin relative to the

parental SA113 strain (Figure 5A) but found that there was no difference in susceptibility with

ZnO NPs (Figure 5B). This indicates that electrostatic interactions do not mediate ZnO NP

toxicity under our assay conditions.
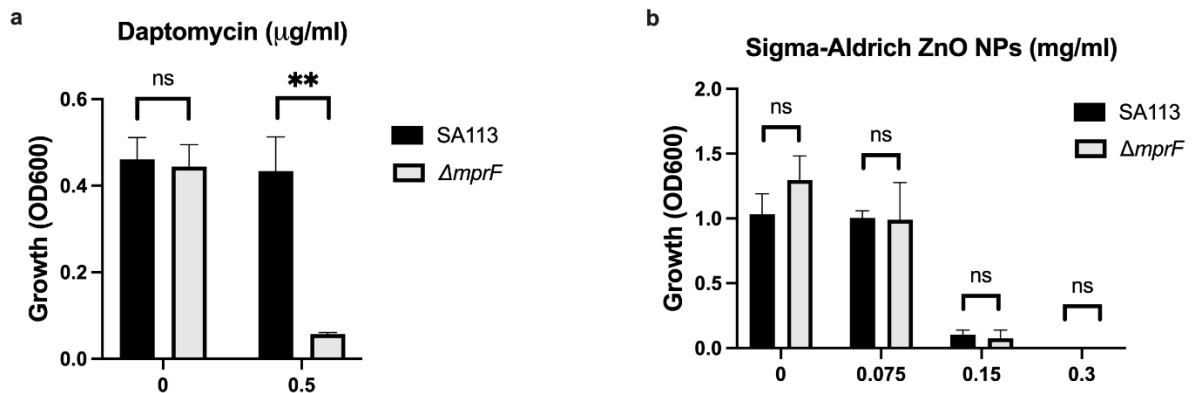
Figure 5. Electrostatic interactions with the bacterial membrane do not mediate ZnO NP toxicity. Parental (SA113) and Δ*mprF S. aureus* growth in a) daptomycin and b) Sigma-Aldrich ZnO NPs. Data are presented as mean +/- SD of at least three independent trials. Statistical significance determined by unpaired t-test; *,p<0.05 or non-significant (ns) from parental levels within each treatment group.

Physical contact is not necessary for ZnO-mediated growth inhibition.

Although electrostatic interactions between bacterial and ZnO NP surfaces did not

mediate toxicity, it is possible that physical contact and disruption of the membrane occur

independent of electrostatic interactions. To evaluate the necessity of physical contact, we

conditioned the media by incubating ZnO NPs in MHB in clear conical tubes for up to 2 months, allowing any soluble factors produced by ZnO NPs to accumulate in the media. ZnO NPs were then removed via centrifugation at the indicated times and the ZnO-free, conditioned supernatant was evaluated for the ability to inhibit bacterial growth (Figure 6A). No statistically significant difference in *S. aureus* growth was seen between unconditioned MHB and conditioned MHB after one day of conditioning (Figure 6A, upper left panel), but by two weeks the ZnO NP-conditioned media exhibited partial growth inhibition (Figure 6A, upper right panel). At one-month, only small amounts of growth were seen in conditioned media although it was not significantly different than the negative control lacking *S. aureus* (Figure 6A, lower left panel). By two months, no growth was seen when *S. aureus* was added to conditioned media (Figure 6A, lower right panel). This suggests that ZnO NPs release a soluble species in a time-dependent manner that contributes to bacterial growth inhibition.

We next wanted to investigate whether physical contact was necessary in a real-time assay as it is possible that physical interactions are more critical for toxicity when time is limited (i.e., there is not a month to generate sufficient soluble species for growth inhibition). To do this, we sequestered Sigma Aldrich ZnO NPs inside a dialysis button covered with dialysis tubing which created a semi-permeable membrane that allowed for diffusion of small soluble species across the membrane but prevented any physical contact between the ZnO NPs and bacteria. To ensure that ZnO NPs were unable to diffuse through the dialysis tubing, sequestered ZnO NPs were first incubated in MHB in the absence of bacteria. We found no change in turbidity relative to MHB alone indicating the ZnO NPs remained inside the dialysis membrane (data not shown). We next added *S. aureus* to the assay and found that the sequestered ZnO NPs effectively inhibited bacterial growth relative to the *S. aureus* grown in the absence of any ZnO NPs (Figure 6B). This confirmed that ZnO NP could inhibit bacterial growth in the absence of physical

interaction with the cell. To compare the effectiveness of growth inhibition in the absence and presence of physical contact, *S. aureus* was also incubated with free (non-sequestered) ZnO NPs under the same conditions. We found that while there was no statistical difference in *S. aureus* growth between 20 mg/ml sequestered and 20 mg/ml free ZnO NPs, only the growth inhibition with the free ZnO NPs showed no statistical difference from our negative control (MHB containing an empty dialysis button but no *S. aureus*). Additionally, we found that there was a statistically significant difference between the 10 mg/ml sequestered ZnO NPs and 10 mg/ml free ZnO NPs. Together, this suggests that while physical contact with Sigma-Aldrich ZnO NPs is not required for growth inhibition in our assay, it still contributes to the effectiveness of the particles.

Figure 6. Sigma Aldrich ZnO NP-mediated growth inhibition is not dependent on physical contact. a) *S. aureus* (SA) Newman growth in unconditioned MHB or MHB conditioned with Sigma-Aldrich ZnO NPs for the indicated amounts of time. b) *S. aureus* Newman growth in MHB containing no ZnO NPs, free ZnO NPs, or ZnO NPs (Sigma-Aldrich) sequestered by a dialysis button. The negative control (Neg Ctrl) represents an empty dialysis button incubated in the absence of S. aureus. Data are presented as mean +/- SD of at least three independent trials. Statistically significant differences are represented by different letters as determined by a one-way ANOVA followed by Tukey's *post hoc* test.

Although we observed that physical contact was not necessary for Sigma-Aldrich NPs to exert their antibacterial effect, we wanted to determine whether this was more broadly true of NPs as a whole or specific to the Sigma-Aldrich NPs. To investigate this, we repeated the same conditioned media and dialysis button experiments with Zochem NPs. Although media conditioned with Zochem NP for up to two months was able to inhibit bacterial growth, it never achieved full inhibition suggesting that it releases less of the soluble species or that it is released at a slower rate (Fig. 7a). The results from Zochem dialysis button assay support this as there is significantly less growth inhibition at 20 mg/ml sequestered ZnO, as compared to Sigma-Aldrich and no growth inhibition at 10 mg/ml sequestered ZnO (Fig. 7B).
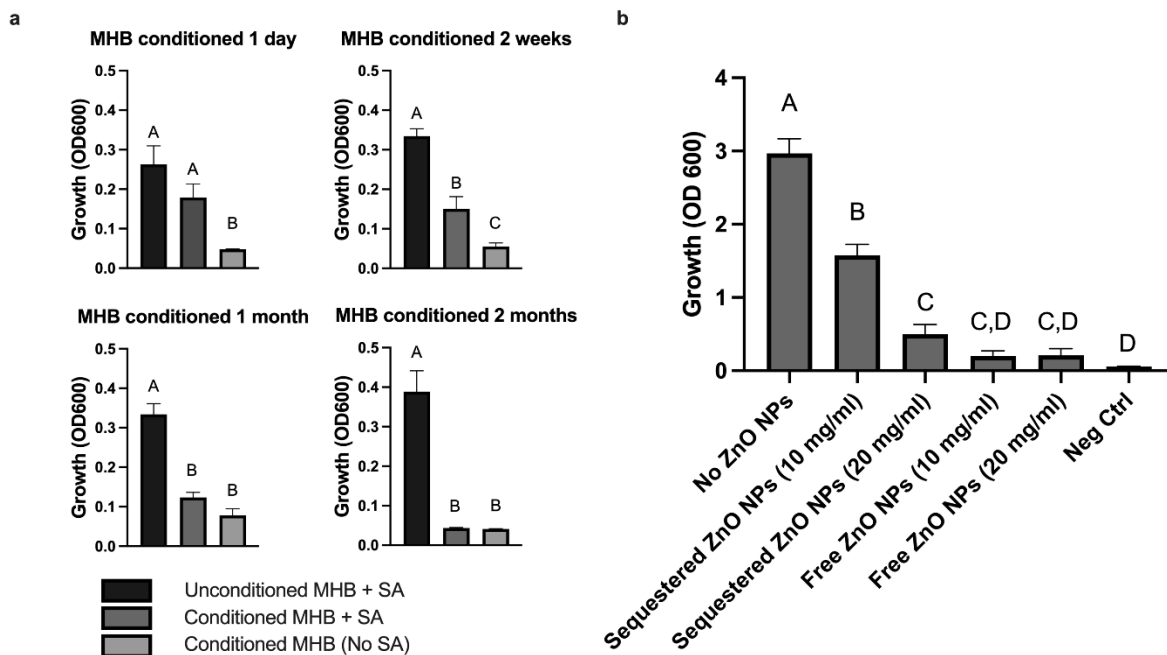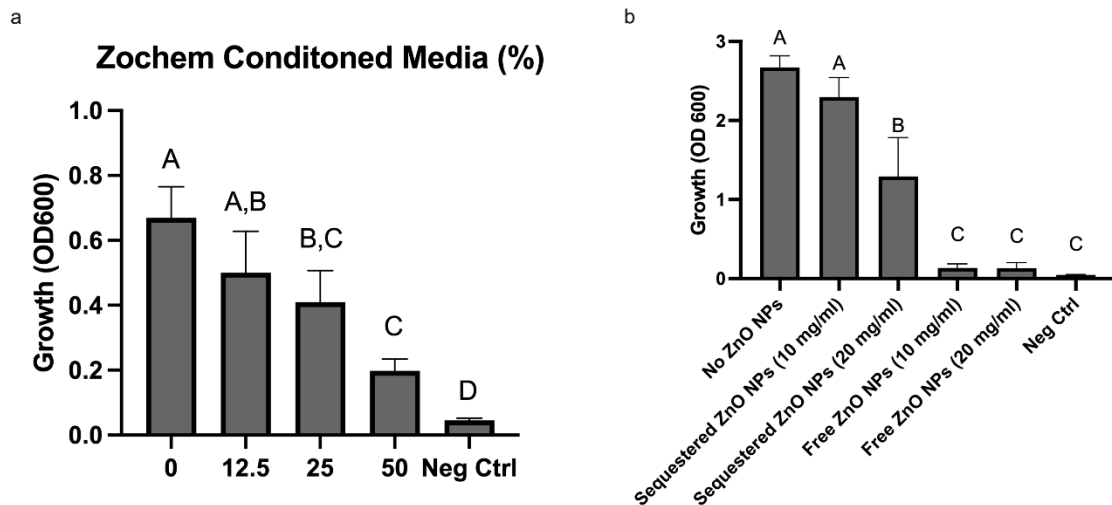

Figure 7. Zochem ZnO NP-mediated growth inhibition is not dependent on physical contact. a) *S. aureus* Newman growth in MHB conditioned with Zochem ZnO NPs for 2 months. b) *S. aureus* Newman growth in MHB containing no ZnO NPs, free ZnO NPs, or ZnO NPs (Zochem) sequestered by a dialysis button. The negative control (Neg Ctrl) represents an empty dialysis button incubated in the absence of *S. aureus*. Data are presented as mean +/- SD of at least three independent trials. Statistically significant differences are represented by different letters as determined by a one-way ANOVA followed by Tukey's *post hoc* test.

Zn^{2+} cations are responsible for soluble ZnO NP toxicity.

Although we saw no difference in growth between the parental *S. aureus* and Δ*katA* in the presence of ZnO-NPs (Figure 4B), we wanted to further confirm that H$_2$O$_2$ is not the soluble

species by incubating ZnO NP-conditioned media with the catalase-deficient *S. aureus* strain. Unsurprisingly, we saw no difference in growth between the parental *S. aureus* and Δ*katA* in the presence of conditioned media (Fig 8A).
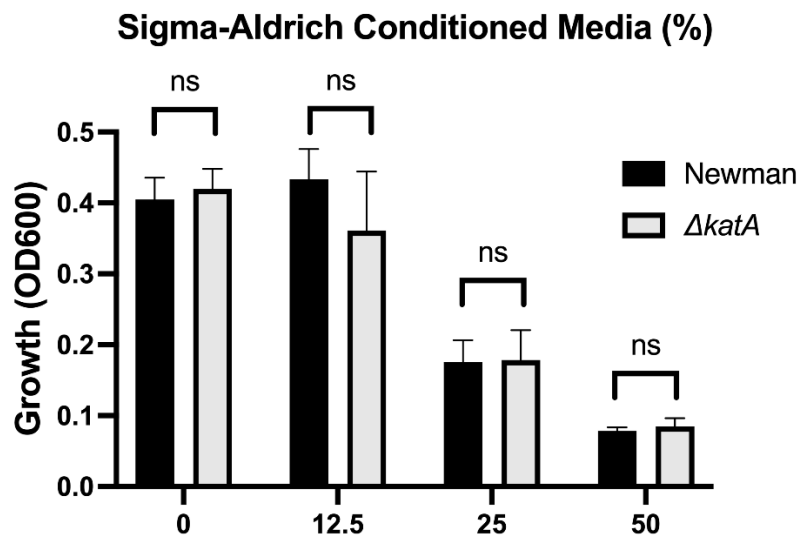
Sigma-Aldrich Conditioned Media (%)

Figure 8. H₂O₂ does not mediate conditioned media toxicity. Parental Newman and Δ*katA* S. aureus growth in media with Sigma-Aldrich ZnO NPs. Error bars represent the mean +/- SD of at least three independent trials. Data are presented as mean +/- SD of at least three independent trials. Statistical significance determined by unpaired t-test; non-significant (ns) from parental levels within each treatment group.

Previous studies have shown dissolution of Zn^{2+} ions from ZnO NP surfaces that have been linked to microbial toxicity (de Lucas-Gil et al., 2019; Gudkov et al., 2021; Lallo Da Silva et al., 2019; Pasquet et al., 2014; Siddiqi et al., 2018; Sirelkhatim et al., 2015; Song et al., 2020). To assess whether accumulation of Zn^{2+} ions in the conditioned media is the soluble factor responsible for growth inhibition, we used Chelex beads to strip the conditioned media of all divalent cations. *S. aureus* grows well in unconditioned MHB (Figure 9, black bar) but the removal of all divalent cations in chelated unconditioned MHB completely inhibits growth (Figure 9, left dark gray bar). This was expected since the presence of some divalent ions is necessary for bacterial growth. As additional negative controls, we incubated *S. aureus* in ZnO NP-conditioned MHB (Figure 9, middle dark gray bar) and chelated conditioned MHB (Figure 9,

26

right dark gray bar) and no growth was seen in either condition. We next supplemented our

experiments with a small amount (25% of total volume) of regular (non-chelated, unconditioned)

MHB to restore enough divalent cations to support the growth of *S. aureus* in the media. When

we supplemented the chelated MHB with regular MHB (Figure 9, left light gray bar), it resulted

in growth that was no different than our positive control (Figure 9, black bar). However,

supplementing with regular MHB was not sufficient for growth when conditioned MHB was

included in place of chelated MHB (Figure 9, middle light gray bar) suggesting the presence of a

toxic, soluble species only present in conditioned media. Chelating conditioned MHB completely

removed this toxic substance resulting once more in full growth of *S. aureus* (Figure 9, right light

gray bar) that was no different from our positive control (black bar). Removal of the toxic

soluble species through chelation indicates that the toxicity is mediated by divalent cations.

MHB	+	-	-	-	+	+	+
Chelated MHB	-	+	-	-	+	-	-
Conditioned MHB	-	-	+	-	-	+	-
Chelated Conditioned MHB	-	-	-	+	-	-	+
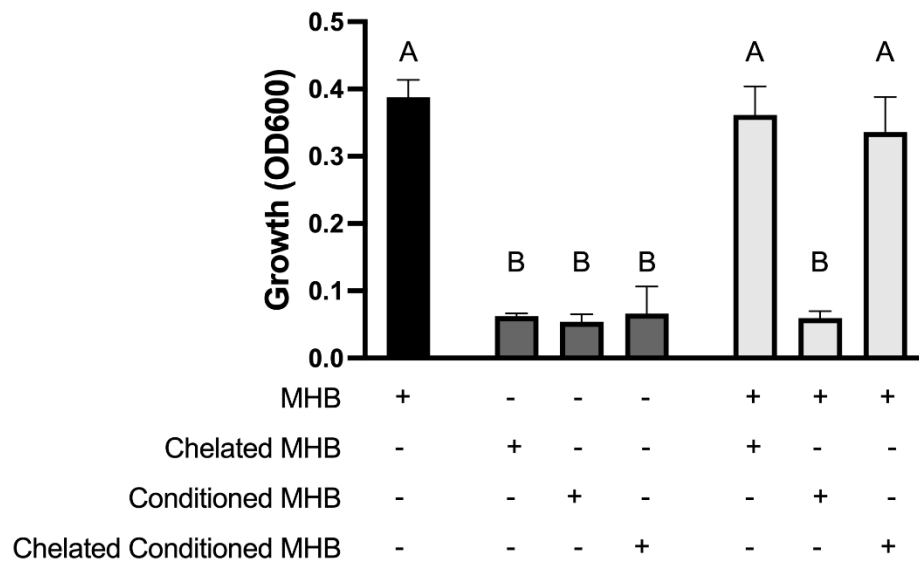
Figure 9. Zn^{2+} ions mediate toxicity. Growth of *S. aureus* Newman in 100% MHB (black bar) or 100% chelated MHB, 100% conditioned media, or 100% chelated conditioned media (dark grey bars) as indicated by the plus (+) sign in the chart. Growth of *S. aureus* in a mixture of 25% MHB and either 75% chelated MHB, 75% conditioned MHB, or 75% chelated conditioned MHB (light grey bars) as indicated by the two plus (+) signs in the chart. Data are presented as mean +/- SD of at least three independent trials. Statistically significant differences are represented by different letters as determined by a one-way ANOVA followed by Tukey's *post hoc* test.

To confirm that Zn^{2+} concentration is increased when MHB is conditioned with ZnO NPs, we measured its concentration using ICP-MS. We found that Zn^{2+} concentration increased 100x after one-day of conditioning (30 μM to 3300μM) and 300x after at least 1 month of conditioning (30 uM to 10000 μM) and that this was reversed after chelation (Table 7). We next evaluated susceptibility of *S. aureus* Newman to Zn^{2+} and found that the

Table 7. Zn^{2+} concentration in media (mean ± SD).

Media Conditions	Zn^{2+} concentration (μM)
MHB	30 ± 8
MHB conditioned 1 day	$3,300 \pm 100$
MHB conditioned ≥1 month	$10,000 \pm 1,000$
MHB conditioned ≥1 month and chelated	20 ± 20

MIC of ZnCl₂ and ZnSO₄ were 0.625 mg/ml (4590 μM) and 1.25mg/ml (9180 μM) respectively (Figure 10A and 10B). It is therefore not surprising that using conditioned media containing Zn^{2+} at similar concentrations completely inhibited growth. To determine whether this was the result of an overabundance of divalent cations or if it was specific to Zn^{2+}, we conducted an MIC with MgCl₂ and saw no inhibition of growth up to 10 mg/ml (Figure 10C). Together this suggests that it is the accumulation of Zn^{2+} ions released from ZnO NP surfaces that are mediating the antibacterial mechanism of ZnO NPs in MHB.
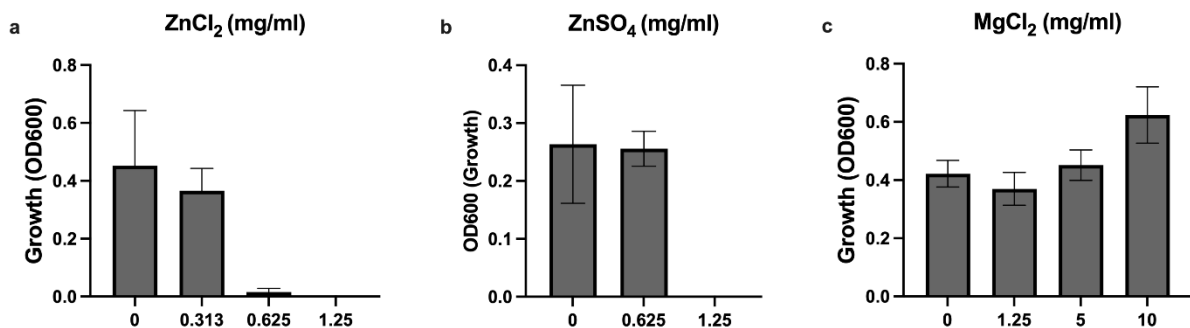

Figure 10. ZnCl₂ and ZnSO₄ but not MgCl₂ inhibits growth. Growth of *S. aureus* Newman in a) ZnCl₂ b) ZnSO₄ and c) MgCl₂. a-c) Data are presented as mean +/- SD of at least three independent trials.

Additional passage of ZnO^R strains failed to generate resistance to Zn^{2+} ions

In light of our findings that physical contact is not necessary and that Zn^{2+} mediates ZnO NP toxicity, we wanted to determine if the intermediately resistant strains would have any resistance to ZnCl$_2$ and conditioned media. We found that even after the ZnO^R strains had been passed a second time under sublethal concentrations of ZnO, they were not resistant to ZnCl$_2$, Sigma-Aldrich conditioned media, or Zochem conditioned media, as compared to the parental strain (Fig. 11A and Fig. 11B). This suggests that a secondary mechanism may contribute to ZnO NP toxicity, although results are difficult to interpret given the intermediate resistance displayed by these strains.
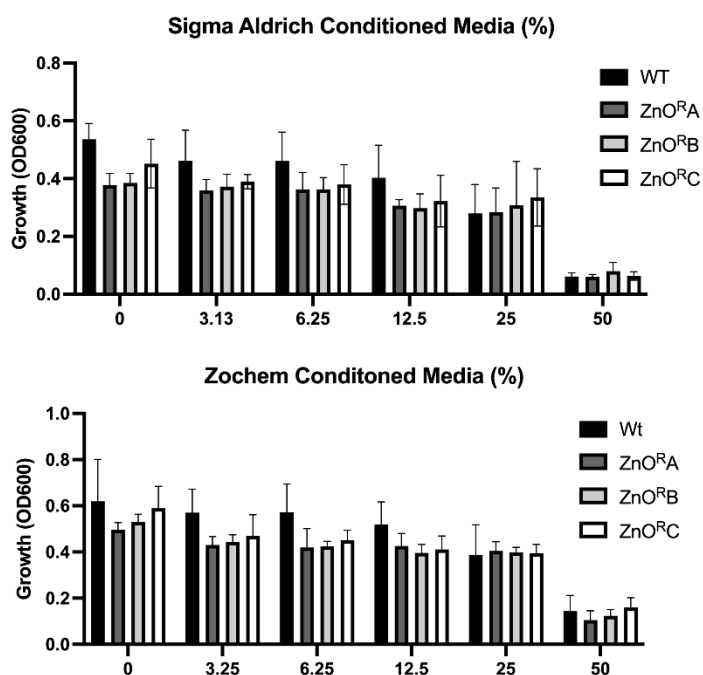
Figure 11. ZnO^R strains do not exhibit resistance to conditioned media Growth of parental and ZnO^R A, B, and C *S. aureus* in a) Sigma-Aldrich conditioned media and b) Zochem conditioned media. a-b) Error bars represent mean +/- SD of at least three independent trials.

Now that we had identified the soluble species as Zn^{2+}, we wanted to again look at the potential impact of electrostatic changes to the bacterial membrane using the Δ*mprF* mutant. However, we saw no difference with either our conditioned media (Figure 12A) or Zn^{2+} generated from ZnCl$_2$ (Figure 12B). Therefore, while electrostatic interactions may still play a role, they are distinct from what is observed with cationic molecules such as antimicrobial peptides or daptomycin and changes in cell membrane surface charge are not sufficient to effect changes in bacterial susceptibility to Zn^{2+}.

Figure 12. Electrostatic interactions with the bacterial membrane do not mediate Zn^{2+} toxicity. Parental SA113 and $\Delta mprF$ *S. aureus* growth in a) Sigma-Aldrich conditioned media, and b) $ZnCl_2$. Data are presented as mean +/- SD of at least three independent trials. St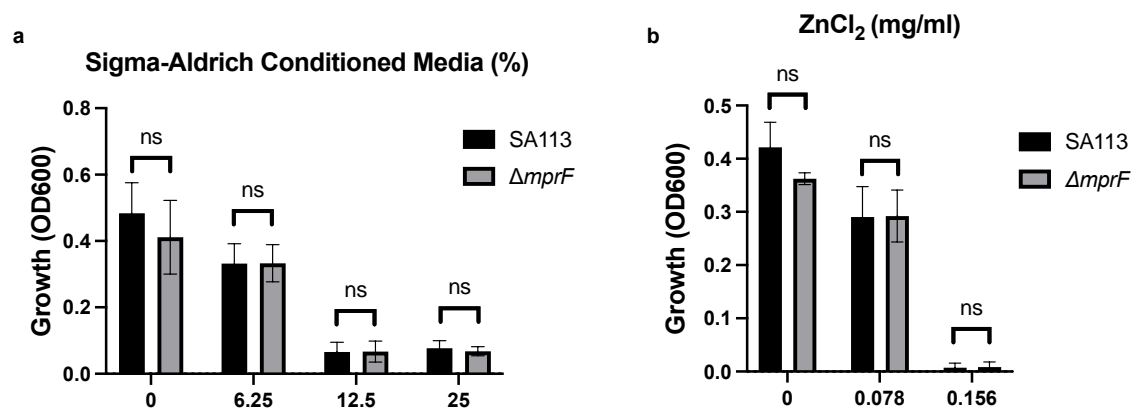atistical significance was determined by unpaired t-test; non-significant (ns) from parental levels within each treatment group.

Zn^{2+} dissolution is highly dependent on both the ZnO NP surface as well as interactions with the media (Li et al., 2011; Herrmann et al., 2014; Pasquet et al., 2014; Joe et al., 2017; Johnson et al., 2022). Several studies have shown that Zn^{2+} dissolution occurs at a higher rate in media (nutrient broth, Luria-Bertani, or MHB) than in water and they speculate that the presence of proteins or other ionic components are increasing the solubility of ZnO (Li et al., 2011; Pasquet et al., 2014; Joe et al., 2017). To investigate the impact of media type on our particles, we performed Sigma-Aldrich ZnO NP survival assays in MHB, PBS, and saline. We observed that ZnO NPs behave bacteriostatically in MHB, however, they behave bacteriocidally in saline and PBS (Fig 12A). Additionally, the ZnO NPs seem to have a stronger bacteriocidal effect in the saline as compared to the PBS. This suggests that the media may influence the release of Zn^{2+} from the NP surface or may otherwise modify the antibacterial ability. To further investigate the effect of media on the antibacterial action, we compared the ability of 50% Sigma-Aldrich conditioned MHB, saline, and PBS. Surprisingly, we found that only conditioned MHB, and not conditioned saline or PBS was able to inhibit bacterial growth (Fig. 13B).

Preliminary data also indicated that the presence of *S. aureus* in the media increases the release

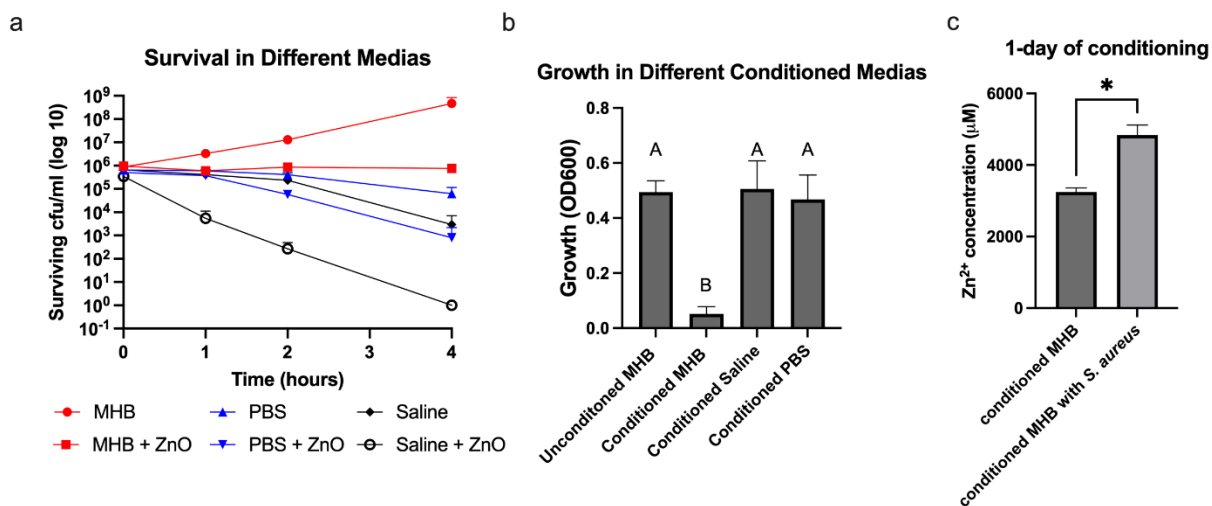of Zn^{2+} from the NP surface in MHB (Fig. 13C).

Figure 13. Media influences ZnO and conditioned media killing. a) Survival of *S. aureus* in MHB, PBS, saline alone and MHB, PBS, and saline with 20 mg/ml ZnO NPs (Sigma-Aldrich). b) Growth of *S. aureus* in unconditioned MHB and 50% MHB plus 50% conditioned MHB, conditioned saline, or conditioned PBS (conditioned with Sigma-Aldrich ZnO NPs). Data is presented as mean +/- SD of at least three independent trials. Statistically significant differences are represented by different letters as determined by a one-way ANOVA followed by Tukey's *post hoc* test. c) Zn^{2+} concentration after 1 day of ZnO NP conditioning with and without *S. aureus*. Data represents mean +/- SD of two independent trials. *, $p < 0.05$ by unpaired t-test.

Discussion

Traditionally antibiotics are small molecules that inhibit a single target essential to

bacterial survival or replication. Due to its high specificity to a conserved target, it can be easy

for bacteria to gain resistance to these kinds of antibiotics because it often requires a single

mutation to change the protein in a way that prevents binding of the antibiotic (Hutchings,

Truman, & Wilkinson, 2019). For this reason, physicians have begun to prescribing antibiotic

cocktails that contain multiple antibiotics with different molecular targets (Russ & Kishony,

2018). By targeting multiple structures simultaneously, it makes it more difficult for bacteria to

gain resistance to each of the cocktail's components. However, it is possible that ZnO NPs can

31

be used to this same effect as it has been proposed that ZnO acts through multiple independent mechanisms and targets non-specific cellular targets (Lallo Da Silva et al., 2019; Slavin et al., 2017). Our attempts to select for resistance to ZnO NPs tentatively supports this theory, as we only saw a moderate and unstable increase in MIC after passage in sublethal ZnO NPs. Supporting this conclusion, the ZnO^R strains also did not display an increase in resistance to ZnO-conditioned media, which suggests more than one toxicity mechanism could be at play. Despite the inability to generate a stable ZnO^R mutant, the high dN/dS ratios, suggests that selection may have occurred on the strains and allow us to make tentative suggestions about which of the proposed mechanisms are involved in ZnO toxicity. Although we were able to tentatively identify a common trend of genes in which SNPs were more highly concentrated, further research is needed to experimentally confirm the roles of identified genes in resistance to ZnO. Specifically, future studies should focus on understanding whether these SNPs result in changes in gene expression, or loss/change of function. Obscuring this, we also observed a high dS/dN ratio for the parental strain of *S. aureus* suggesting that other environmental pressures outside of ZnO may have resulted in selection at the identified loci.

Production of ROS, particularly H_2O_2, has long been a prevailing theory of ZnO NP-mediated toxicity with multiple studies directly measuring ROS production by ZnO NPs (S. Liu et al., 2019; Soltanian et al., 2021; Tiwari et al., 2018; X. Xu et al., 2013). The bigger question is the biological significance of this ROS production. Some studies have seen evidence of lipid peroxidation, which they have attributed to ZnO-mediated ROS generation (Eid, Sayed, Hozayen, & Dishisha, 2023), although other studies report an absence of lipid peroxidation (Kadiyala et al., 2018). Further confounding the role of ROS, several studies have reported no increase in the expression of oxidative stress genes in response to exposure to ZnO NPs (Kadiyala et al., 2018; Pati et al., 2014; Raghupathi et al., 2011). We used *S. aureus* with a

deletion in the catalase gene, *katA*, to directly examine whether H_2O_2 production by ZnO NPs mediates toxicity. Loss of *katA* significantly increases *S. aureus* susceptibility to H_2O_2 (Park et al., 2008) and Figure 4A), yet no change in growth was seen when $\Delta katA$ was exposed to ZnO relative to the parental strain (Figure 4B). These findings align with gene expression studies that found that ZnO NPs do not induce *katA* expression in *S. aureus* (Kadiyala et al., 2018; Pati et al., 2014; Raghupathi et al., 2011). Although it is possible that ROS other than H_2O_2 contribute to toxicity, Kadiyala et al., 2018 showed that the powerful antioxidant N-acetylcysteine provided no protective effects against ZnO-NPs (Kadiyala et al., 2018), which provides some evidence that our findings may extend beyond H_2O_2. Additionally, the lack of mutated genes involved in defense against ROS that arose in the ZnO^R mutants may suggest more broadly that ROS production is not the predominant mechanism of action. We will note that our results contradict those of Borda et al. who found a correlation between H_2O_2 and ZnO NP susceptibility using bacterial species with differing H_2O_2 sensitivities (Borda d' Água et al., 2018). However, this approach cannot control for other variables that would differ between species beyond that of H_2O_2 susceptibility. A benefit of using an isogenic mutant is that the only difference between the strains is loss of the *katA* gene and thus any changes in susceptibility can be directly attributable to H_2O_2. Although we see no evidence of H_2O_2 involvement in ZnO NP toxicity in our assay conditions, properties of ZnO NPs can differ widely depending on their method of synthesis, physical characteristics, and assay conditions including media type or the presence or absence of light (de Lucas-Gil et al., 2019; M. Li et al., 2011; X. Xu et al., 2013). Therefore, while we cannot rule out the role of H_2O_2 in mediating ZnO toxicity under any condition, it is not a universal mechanism.

Physical contact and/or internalization are additional mechanisms attributed to ZnO NPs (Lallo Da Silva et al., 2019; Sirelkhatim et al., 2015). We previously investigated the role of

internalization in ZnO-mediated toxicity using microparticles incapable of being internalized and found that ZnO still inhibited *S. aureus* growth (Johnson et al., 2022). However, this does not rule out the necessity of physical contact in disruption of the cell envelope. Membrane damage after contact with ZnO NPs has been reported using SEM or TEM images (Akbar et al., 2019; Dhanasegaran et al., 2022; Joe et al., 2017; Johnson et al., 2022; Y. Liu et al., 2009; Manzoor et al., 2016; Reeks et al., 2021; Siddiqi et al., 2018). Several means of interaction have been proposed including the role of proteins and polysaccharides mediating attachment (Dhanasegaran et al., 2022) as well as electrostatic interactions (Arakha et al., 2015; Feris et al., 2010). Although we saw no evidence of electrostatic interactions with ZnO NPs (Figure 5B), previous studies concluded that ZnO NPs with positive surface potentials have higher toxicity than synonymous ZnO NPs with negative surface potentials (Arakha et al., 2015; Feris et al., 2010). The ZnO NPs used in our assays have a negative net surface potential as measured by Zeta potential measurements (data not shown) and therefore it is possible that electrostatic interactions could be seen with ZnO NPs having a more positive surface potential. Nonetheless, our results with $ZnCl_2$ indicate that changes in cell membrane surface charge is not sufficient to effect changes in bacterial susceptibility to Zn^{2+} itself (Figure 12B).

Despite the evidence of membrane damage after ZnO NP exposure (Akbar et al., 2019; Dhanasegaran et al., 2022), our results indicate that physical contact may not be strictly necessary for ZnO-mediated toxicity. Few studies have evaluated ZnO cytotoxicity in the absence of physical contact and it is possible that damage to the cell membrane may occur through a mechanism independent of physical contact. We find that soluble Zn^{2+} accumulates in MHB over time leading to bacterial growth inhibition and that this toxicity can be reversed by removal of Zn^{2+} (Figure 9A and Table 7). This inhibition is also seen in real-time when 20 mg/ml of ZnO NPs are physically separated from bacterial cells by a membrane permeable to

soluble species but not the particles themselves (Figure 6B). However, although we see

significant inhibition with sequestered ZnO NPs at 20 mg/ml, there is still more growth relative

to the negative control than is seen with free (non-sequestered) ZnO NPs. Additionally, free ZnO

NPs at 10 mg/ml completely inhibited bacterial growth while sequestered ZnO NPs at the same

concentration did not. Therefore, while physical contact may not be necessary, it could still

contribute to toxicity.

      Our results point to Zn^{2+} ions, rather than H_2O_2, as the soluble species mediating ZnO NP

toxicity. Even in the absence of a strong phenotype, it is possible that the selection was due to the

selective pressures ZnO placed on *S. aureus*. Zn^{2+} toxicity may occur through two mechanisms:

1) mis-metalation of enzymes that require metal cofactors leading to protein dysfunction and 2)

disruption of osmotic homeostasis (de Lucas-Gil et al., 2019; Gudkov et al., 2021; Lemire,

Harrison, & Turner, 2013; Siddiqi et al., 2018; Sirelkhatim et al., 2015; Song et al., 2020). While

the exact role of Zn^{2+} in cytotoxicity is still unconfirmed, the ability of Zn^{2+} ions to induce

bacterial death has been established (Lemire et al., 2013; McDevitt et al., 2011). Despite this,

there is relatively little known about the molecular targets. McDevitt et al. reports that Zn^{2+}

inhibits acquisition of Mn^{2+} by competing for binding to the solute binding protein PsaA, causing

Mn^{2+} starvation, growth inhibition, and susceptibility to oxidative stress (McDevitt et al., 2011).

Enzymes that contain sulfhydryl moieties are also likely to be the biological targets of soft

metals such as zinc (F. F. Xu & Imlay, 2012). These moieties are commonly found in

dehydratase-family enzymes that are directly involved in catalysis of key metabolic pathways,

and their inactivation can arrest growth. However, Zn^{2+} could potentially competitively bind with

many different metal-binding moieties as 30% to 50% of proteins are predicted to be dependent

on metal atoms for their structure and function (Andreini, Bertini, & Rosato, 2004). Although the

SNP analysis did not reveal mutations in PsaA, or other obvious targets related to Zn^{2+} toxicity

such as metal transporters, SNPs seemed to accumulate in non-phage encoded genes with GO terms associated with metal cation binding. This was particularly true of DNA binding proteins, supporting the hypothesis that accumulation of Zn^{2+} ions causes mis-metalation of enzymes involved in DNA replication and regulation resulting in bacterial death.

Zn^{2+} dissolution is highly dependent on both the ZnO NP surface as well as interactions with the media (Herrmann, García-García, & Reller, 2014; Joe et al., 2017; Johnson et al., 2022; M. Li et al., 2011; Pasquet et al., 2014). Several studies have shown that Zn^{2+} dissolution occurs at a higher rate in media (nutrient broth, Luria-Bertani, or MHB) than in water and they speculate that the presence of proteins or other ionic components are increasing the solubility of ZnO (Joe et al., 2017; M. Li et al., 2011; Pasquet et al., 2014). This aligns with our observation that the presence of *S. aureus* increases Zn^{2+} release from ZnO and may explain why we observe toxicity of ZnO NPs after 1 day when NPs are incubated with *S. aureus*, but do not see toxicity of ZnO NP conditioned media until later time points. Despite increasing the rate of release, the presence of soluble components such as phosphates, Na^+, Fe^+, and some organic molecules also decrease toxicity of Zn^{2+} after its release (Herrmann et al., 2014; Johnson et al., 2022; M. Li et al., 2011; Pasquet et al., 2014; Song et al., 2020). As Zn^{2+} is released from the surface of ZnO NPs, it is possible that it becomes bound by organic components in the MHB and is unable to accumulate intracellularly to inhibit bacterial growth. This may explain why we observed that ZnO NPs behave bacteriostatically in MHB at short time points. It is possible that, at longer time points, such as with the conditioned media experiments, the organic molecules become saturated with Zn^{2+}, and free Zn^{2+} accumulates in the media and causes bacterial toxicity.

Interestingly, ZnO NPs behave very differently in PBS and saline than they do in media. PBS and saline are both relatively simple medias that lack any organic components, allowing Zn^{2+} to accumulate relatively quickly in the media (M. Li et al., 2011; Song et al., 2020). As a

result, ZnO NPs behave bacteriocidally in PBS and saline. In alignment with Li et al. which reported that the presence of phosphate in solution increases the Zn^{2+} release profile but decreased ZnO toxicity as Zn^{2+} reacts with phosphates to form innocuous zinc phosphate crystals, we found that ZnO NPs in saline have stronger bactericidal action than PBS. We hypothesize this is due to the formation of innocuous zinc phosphate crystals in PBS that decrease the concentration of free Zn^{2+}. What is less clear is why the PBS and saline conditioned with ZnO NPs did not possess any antimicrobial activity. One possible explanation for this may be that MHB added to the conditioned PBS and saline to provide nutrients during the growth assay also provides organic substrates that bind and detoxify free Zn^{2+} present in the media. Further experimentation will be needed to determine how these media-types are affecting Zn^{2+} dissolution and toxicity.

The presence and nature of surface defects, which are tied to various particle properties such as size, morphology, and synthesis conditions, also influence the ability of ZnO particles to release Zn^{2+} (de Lucas-Gil et al., 2019; Johnson et al., 2022; Song et al., 2020). This aligns with our observation that the Alfa Aesar NPs that share similar size and morphological properties as Sigma-Aldrich also share similar toxicity, while Zochem particles which are larger with fewer surface defects and a smaller surface area, display decreased toxicity as compared to Sigma-Aldrich NPs. We speculate that this difference in toxicity may be proportional to the differences in Zn^{2+} release between Sigma-Aldrich and Zochem ZnO. We previously found that there exist relevant morphological differences in the form of an increased abundance of surface trap states related to oxygen deficiencies at the polar surfaces of ZnO microparticles, which indicates an excess of Zn^{2+} ions at these surfaces that can be released into solutions (Johnson et al., 2022). In light of this, it may be possible to modify ZnO NPs to enhance their bacterial growth inhibition. This can be done during synthesis via alternate synthesis methods (Ralphs, Hardacre, & James,

2013; Su et al., 2017; Xia et al., 2014), conditions (Asok, Gandhi, & Kulkarni, 2012; Xing et al., 2010), precursors (Guo et al., 2015; Wang et al., 2012), or the addition of dopants (Gao et al., 2016; V & Vijayaraghavan, 2017) all of which can impart desirable morphologies and chemical properties. Post synthesis treatment is also a viable method for improving the antibacterial activity as annealing in anaerobic environments and surface functionalization can modify the surface defect structure potentially leading to increased Zn^{2+} release (Cui et al., 2012; Elhaj Baddar, Matocha, & Unrine, 2019; Laurenti, Stassi, Canavese, & Cauda, 2017; Lv et al., 2013).

A challenge in studying ZnO NP-mediated bacterial toxicity is the extensive variability in particle morphology, media type, and even experimental conditions such as the presence or absence of light, all of which can interact and potentially have profound effects on activity (de Lucas-Gil et al., 2019; Joe et al., 2017; M. Li et al., 2011; Pasquet et al., 2014; Song et al., 2020; X. Xu et al., 2013). This demonstrates the need for extensive characterization of the nanoparticles, as well as standardized test conditions when studying the mechanism of ZnO toxicity. It also may explain the contradictory findings regarding the production of ROS, dissolution of Zn^{2+}, and necessity of physical contact in ZnO NP-mediated toxicity. Our own assays were all performed in MHB largely because MHB has historically been the standard media for MIC assays, but it is important to note that our results may be specific to MHB, and the mechanism of action could vary with other media or particle types. Additional work investigating this interplay will be critical for maximizing the antibacterial activity of ZnO NPs and optimizing their use in future applications.

References

Akbar, A., Sadiq, M. B., Ali, I., Muhammad, N., Rehman, Z., Khan, M. N., . . . Anal, A. K. (2019). Synthesis and antimicrobial activity of zinc oxide nanoparticles against foodborne pathogens Salmonella typhimurium and Staphylococcus aureus. *Biocatalysis and Agricultural Biotechnology, 17*, 36-42. doi:https://doi.org/10.1016/j.bcab.2018.11.005

Ali, S. S., Moawad, M. S., Hussein, M. A., Azab, M., Abdelkarim, E. A., Badr, A., . . . Khalil, M. (2021). Efficacy of metal oxide nanoparticles as novel antimicrobial agents against multi-drug and multi-virulent Staphylococcus aureus isolates from retail raw chicken meat and giblets. *Int J Food Microbiol, 344*, 109116. doi:10.1016/j.ijfoodmicro.2021.109116

Andreini, C., Bertini, I., & Rosato, A. (2004). A hint to search for metalloproteins in gene banks. *Bioinformatics, 20*(9), 1373-1380. doi:10.1093/bioinformatics/bth095

Antibiotic resistance threats in the United States, 2019. (2019). Retrieved from https://stacks.cdc.gov/view/cdc/82532

Arakha, M., Saleem, M., Mallick, B. C., & Jha, S. (2015). The effects of interfacial potential on antimicrobial propensity of ZnO nanoparticle. *Scientific Reports, 5*(1), 9578. doi:10.1038/srep09578

Asok, A., Gandhi, M. N., & Kulkarni, A. R. (2012). Enhanced visible photoluminescence in ZnO quantum dots by promotion of oxygen vacancy formation. *Nanoscale, 4*(16), 4943-4946. doi:10.1039/C2NR31044A

Borda d' Água, R., Branquinho, R., Duarte, M. P., Maurício, E., Fernando, A. L., Martins, R., & Fortunato, E. (2018). Efficient coverage of ZnO nanoparticles on cotton fibres for antibacterial finishing using a rapid and low cost in situ synthesis. *New Journal of Chemistry, 42*(2), 1052-1060. doi:10.1039/C7NJ03418K

Cheung, G. Y. C., Bae, J. S., & Otto, M. (2021). Pathogenicity and virulence of Staphylococcus aureus. *Virulence, 12*(1), 547-569. doi:10.1080/21505594.2021.1878688

Cui, L., Zhang, H.-Y., Wang, G.-G., Yang, F.-X., Kuang, X.-P., Sun, R., & Han, J.-C. (2012). Effect of annealing temperature and annealing atmosphere on the structure and optical properties of ZnO thin films on sapphire (0001) substrates by magnetron sputtering. *Applied Surface Science, 258*(7), 2479-2485. doi:https://doi.org/10.1016/j.apsusc.2011.10.076

Dadi, R., Azouani, R., Traore, M., Mielcarek, C., & Kanaev, A. (2019). Antibacterial activity of ZnO and CuO nanoparticles against gram positive and gram negative strains. *Materials Science and Engineering: C, 104*, 109968. doi:https://doi.org/10.1016/j.msec.2019.109968

de Lucas-Gil, E., Del Campo, A., Pascual, L., Monte-Serrano, M., Menéndez, J., Fernández, J. F., & Rubio-Marcos, F. (2019). The fight against multidrug-resistant organisms: The role of ZnO crystalline defects. *Materials Science and Engineering: C, 99*, 575-581. doi:https://doi.org/10.1016/j.msec.2019.02.004

DeLeo, F. R., & Chambers, H. F. (2009). Reemergence of antibiotic-resistant Staphylococcus aureus in the genomics era. *The Journal of Clinical Investigation, 119*(9), 2464-2474. doi:10.1172/JCI38226

Dhanasegaran, K., Djearamane, S., Liang, S., Ling Shing, W., Kasivelu, G., Lee, P. F., & Lim, Y. (2022). Antibacterial properties of zinc oxide nanoparticles on Pseudomonas aeruginosa (ATCC 27853). *Scientia Iranica, 28*, 3806-3815. doi:10.24200/sci.2021.56815.4974

Eid, A. M., Sayed, O. M., Hozayen, W., & Dishisha, T. (2023). Mechanistic study of copper oxide, zinc oxide, cadmium oxide, and silver nanoparticles-mediated toxicity on the probiotic Lactobacillus reuteri. *Drug Chem Toxicol, 46*(5), 825-840. doi:10.1080/01480545.2022.2104865

Elhaj Baddar, Z., Matocha, C. J., & Unrine, J. M. (2019). Surface coating effects on the sorption and dissolution of ZnO nanoparticles in soil. *Environmental Science: Nano, 6*(8), 2495-2507. doi:10.1039/C9EN00348G

Ernst, C. M., Staubitz, P., Mishra, N. N., Yang, S.-J., Hornig, G., Kalbacher, H., . . . Peschel, A. (2009). The Bacterial Defensin Resistance Protein MprF Consists of Separable Domains for Lipid Lysinylation and Antimicrobial Peptide Repulsion. *PLOS Pathogens, 5*(11), e1000660. doi:10.1371/journal.ppat.1000660

Feris, K., Otto, C., Tinker, J., Wingett, D., Punnoose, A., Thurber, A., . . . Pink, D. (2010). Electrostatic Interactions Affect Nanoparticle-Mediated Toxicity to Gram-Negative Bacterium Pseudomonas aeruginosa PAO1. *Langmuir, 26*(6), 4429-4436. doi:10.1021/la903491z

Fischbach, M. A., & Walsh, C. T. (2009). Antibiotics for emerging pathogens. *Science, 325*(5944), 1089-1093. doi:10.1126/science.1176667

Gao, Q., Dai, Y., Li, C., Yang, L., Li, X., & Cui, C. (2016). Correlation between oxygen vacancies and dopant concentration in Mn-doped ZnO nanoparticles synthesized by co-precipitation technique. *Journal of Alloys and Compounds, 684*, 669-676. doi:https://doi.org/10.1016/j.jallcom.2016.05.227

Gudkov, S. V., Burmistrov, D. E., Serov, D. A., Rebezov, M. B., Semenova, A. A., & Lisitsyn, A. B. (2021). A Mini Review of Antibacterial Properties of ZnO Nanoparticles. *Frontiers in Physics, 9*. doi:10.3389/fphy.2021.641481

Guo, H.-L., Zhu, Q., Wu, X.-L., Jiang, Y.-F., Xie, X., & Xu, A.-W. (2015). Oxygen deficient ZnO1−x nanosheets with high visible light photocatalytic activity. *Nanoscale, 7*(16), 7216-7223. doi:10.1039/C5NR00271K

Heidary, M., Bostanabad, S. Z., Amini, S. M., Jafari, A., Nobar, M. G., Ghodousi, A., . . . Darban-Sarokhalil, D. (2019). The Anti-Mycobacterial Activity Of Ag, ZnO, And Ag-ZnO Nanoparticles Against MDR- And XDR-*Mycobacterium tuberculosis*. *Infection and Drug Resistance, 12*, 3425-3435. doi:10.2147/idr.S221408

Herrmann, R., García-García, F. J., & Reller, A. (2014). Rapid degradation of zinc oxide nanoparticles by phosphate ions. *Beilstein Journal of Nanotechnology, 5*, 2007-2015. doi:10.3762/bjnano.5.209

Hutchings, M. I., Truman, A. W., & Wilkinson, B. (2019). Antibiotics: past, present and future. *Current Opinion in Microbiology, 51*, 72-80. doi:https://doi.org/10.1016/j.mib.2019.10.008

Joe, A., Park, S.-H., Shim, K.-D., Kim, D.-J., Jhee, K.-H., Lee, H.-W., . . . Jang, E.-S. (2017). Antibacterial mechanism of ZnO nanoparticles under dark conditions. *Journal of Industrial and Engineering Chemistry, 45*, 430-439. doi:https://doi.org/10.1016/j.jiec.2016.10.013

Johnson, D., Reeks, J. M., Caron, A., Tzoka, I., Ali, I., McGillivray, S. M., & Strzhemechny, Y. M. (2022). Influence of Surface Properties and Microbial Growth Media on Antibacterial Action of ZnO. *Coatings, 12*(11). doi:10.3390/coatings12111648

Kadiyala, U., Turali-Emre, E. S., Bahng, J. H., Kotov, N. A., & Vanepps, J. S. (2018). Unexpected insights into antibacterial activity of zinc oxide nanoparticles against

methicillin resistant *Staphylococcus aureus* (MRSA). *Nanoscale, 10*(10), 4927-4939. doi:10.1039/c7nr08499d

Kerepesi, C., Szabó, J. E., Papp-Kádár, V., Dobay, O., Szabó, D., Grolmusz, V., & Vértessy, B. G. (2016). Life without dUTPase. *Frontiers in Microbiology, 7*. doi:10.3389/fmicb.2016.01768

Lallo Da Silva, B., Abuçafy, M. P., Berbel Manaia, E., Oshiro Junior, J. A., Chiari-Andréo, B. G., Pietro, R. C. R., & Chiavacci, L. A. (2019). Relationship Between Structure And Antimicrobial Activity Of Zinc Oxide Nanoparticles: An Overview. *International Journal of Nanomedicine, Volume 14*, 9395-9410. doi:10.2147/ijn.s216204

Laurenti, M., Stassi, S., Canavese, G., & Cauda, V. (2017). Surface Engineering of Nanostructured ZnO Surfaces. *Advanced Materials Interfaces, 4*(2), 1600758. doi:https://doi.org/10.1002/admi.201600758

Lemire, J. A., Harrison, J. J., & Turner, R. J. (2013). Antimicrobial activity of metals: mechanisms, molecular targets and applications. *Nature Reviews Microbiology, 11*(6), 371-384. doi:10.1038/nrmicro3028

Li, M., Zhu, L., & Lin, D. (2011). Toxicity of ZnO Nanoparticles to *Escherichia coli*: Mechanism and the Influence of Medium Components. *Environmental Science & Technology, 45*(5), 1977-1983. doi:10.1021/es102624t

Li, Q., Mahendra, S., Lyon, D. Y., Brunet, L., Liga, M. V., Li, D., & Alvarez, P. J. J. (2008). Antimicrobial nanomaterials for water disinfection and microbial control: Potential applications and implications. *Water Research, 42*(18), 4591-4602. doi:https://doi.org/10.1016/j.watres.2008.08.015

Li, Y., Liao, C., & Tjong, S. C. (2020). Recent Advances in Zinc Oxide Nanostructures with Antimicrobial Activities. *International Journal of Molecular Sciences, 21*(22), 8836. Retrieved from https://www.mdpi.com/1422-0067/21/22/8836

Liu, S., Lai, Y., Zhao, X., Li, R., Huang, F., Zheng, Z., & Ying, M. (2019). The influence of H2O2 on the antibacterial activity of ZnO. *Materials Research Express, 6*(8), 0850c0856. doi:10.1088/2053-1591/ab2506

Liu, Y., He, L., Mustapha, A., Li, H., Hu, Z. Q., & Lin, M. (2009). Antibacterial activities of zinc oxide nanoparticles against Escherichia coli O157:H7. *Journal of Applied Microbiology, 107*(4), 1193-1201. doi:10.1111/j.1365-2672.2009.04303.x

Lv, Y., Pan, C., Ma, X., Zong, R., Bai, X., & Zhu, Y. (2013). Production of visible activity and UV performance enhancement of ZnO photocatalyst via vacuum deoxidation. *Applied Catalysis B: Environmental, 138-139*, 26-32. doi:https://doi.org/10.1016/j.apcatb.2013.02.011

Manzoor, U., Siddique, S., Ahmed, R., Noreen, Z., Bokhari, H., & Ahmad, I. (2016). Antibacterial, Structural and Optical Characterization of Mechano-Chemically Prepared ZnO Nanoparticles. *PLOS ONE, 11*(5), e0154704. doi:10.1371/journal.pone.0154704

McDevitt, C. A., Ogunniyi, A. D., Valkov, E., Lawrence, M. C., Kobe, B., McEwan, A. G., & Paton, J. C. (2011). A Molecular Mechanism for Bacterial Susceptibility to Zinc. *PLOS Pathogens, 7*(11), e1002357. doi:10.1371/journal.ppat.1002357

Modi, S., Inwati, G. K., Gacem, A., Saquib Abullais, S., Prajapati, R., Yadav, V. K., . . . Jeon, B.-H. (2022). Nanostructured Antibiotics and Their Emerging Medicinal Applications: An Overview of Nanoantibiotics. *Antibiotics, 11*(6), 708. doi:10.3390/antibiotics11060708

Park, B., Nizet, V., & Liu, G. Y. (2008). Role of *Staphylococcus aureus* Catalase in Niche Competition against *Streptococcus pneumoniae*. *Journal of Bacteriology, 190*(7), 2275-2278. doi:10.1128/jb.00006-08

Pasquet, J., Chevalier, Y., Pelletier, J., Couval, E., Bouvier, D., & Bolzinger, M.-A. (2014). The contribution of zinc ions to the antimicrobial activity of zinc oxide. *Colloids and Surfaces A: Physicochemical and Engineering Aspects, 457*, 263-274. doi:https://doi.org/10.1016/j.colsurfa.2014.05.057

Pati, R., Mehta, R. K., Mohanty, S., Padhi, A., Sengupta, M., Vaseeharan, B., . . . Sonawane, A. (2014). Topical application of zinc oxide nanoparticles reduces bacterial skin infection in mice and exhibits antibacterial activity by inducing oxidative stress response and cell membrane disintegration in macrophages. *Nanomedicine-Nanotechnology Biology and Medicine, 10*(6), 1195-1208. doi:10.1016/j.nano.2014.02.012

Peschel, A., Jack, R. W., Otto, M., Collins, L. V., Staubitz, P., Nicholson, G., . . . van Strijp, J. A. (2001). *Staphylococcus aureus* resistance to human defensins and evasion of neutrophil killing via the novel virulence factor MprF is based on modification of membrane lipids with l-lysine. *J Exp Med, 193*(9), 1067-1076. doi:10.1084/jem.193.9.1067

Preeti, Radhakrishnan, V. S., Mukherjee, S., Mukherjee, S., Singh, S. P., & Prasad, T. (2020). ZnO Quantum Dots: Broad Spectrum Microbicidal Agent Against Multidrug Resistant Pathogens *E. coli* and *C. albicans*. *Frontiers in Nanotechnology, 2*. doi:10.3389/fnano.2020.576342

Raghupathi, K. R., Koodali, R. T., & Manna, A. C. (2011). Size-Dependent Bacterial Growth Inhibition and Mechanism of Antibacterial Activity of Zinc Oxide Nanoparticles. *Langmuir, 27*(7), 4020-4028. doi:10.1021/la104825u

Ralphs, K., Hardacre, C., & James, S. L. (2013). Application of heterogeneous catalysts prepared by mechanochemical synthesis. *Chemical Society Reviews, 42*(18), 7701-7718. doi:10.1039/C3CS60066A

Reeks, J. M., Ali, I., Moss, W. J., Davis, E., McGillivray, S. M., & Strzhemechny, Y. M. (2021). Microscale ZnO with controllable crystal morphology as a platform to study antibacterial action on *Staphylococcus aureus*. *Biointerphases, 16*(3), 031003. doi:10.1116/6.0000957

Russ, D., & Kishony, R. (2018). Additivity of inhibitory effects in multidrug combinations. *Nature Microbiology, 3*(12), 1339-1345. doi:10.1038/s41564-018-0252-1

Sharma, D. K., Shukla, S., Sharma, K. K., & Kumar, V. (2022). A review on ZnO: Fundamental properties and applications. *Materials Today: Proceedings, 49*, 3028-3035. doi:https://doi.org/10.1016/j.matpr.2020.10.238

Siddiqi, K. S., Ur Rahman, A., Tajuddin, & Husen, A. (2018). Properties of Zinc Oxide Nanoparticles and Their Activity Against Microbes. *Nanoscale Research Letters, 13*(1). doi:10.1186/s11671-018-2532-3

Sirelkhatim, A., Mahmud, S., Seeni, A., Kaus, N. H. M., Ann, L. C., Bakhori, S. K. M., . . . Mohamad, D. (2015). Review on Zinc Oxide Nanoparticles: Antibacterial Activity and Toxicity Mechanism. *Nano-Micro Letters, 7*(3), 219-242. doi:10.1007/s40820-015-0040-x

Slavin, Y. N., Asnis, J., Häfeli, U. O., & Bach, H. (2017). Metal nanoparticles: understanding the mechanisms behind antibacterial activity. *Journal of Nanobiotechnology, 15*(1). doi:10.1186/s12951-017-0308-z

Smaoui, S., Chérif, I., Ben Hlima, H., Khan, M. U., Rebezov, M., Thiruvengadam, M., . . . Lorenzo, J. M. (2023). Zinc oxide nanoparticles in meat packaging: A systematic review of recent literature. *Food Packaging and Shelf Life, 36*, 101045. doi:https://doi.org/10.1016/j.fpsl.2023.101045

Soltanian, S., Sheikhbahaei, M., Mohamadi, N., Pabarja, A., Abadi, M. F. S., & Tahroudi, M. H. M. (2021). Biosynthesis of Zinc Oxide Nanoparticles Using Hertia intermedia and

Evaluation of its Cytotoxic and Antimicrobial Activities. *BioNanoScience, 11*(2), 245-255. doi:10.1007/s12668-020-00816-z

Song, K., Zhang, W., Sun, C., Hu, X., Wang, J., & Yao, L. (2020). Dynamic cytotoxicity of ZnO nanoparticles and bulk particles to Escherichia coli: A view from unfixed ZnO particle:Zn2+ ratio. *Aquatic Toxicology, 220*, 105407. doi:https://doi.org/10.1016/j.aquatox.2020.105407

Su, X.-F., Chen, J.-B., He, R.-M., Li, Y., Wang, J., & Wang, C.-W. (2017). The preparation of oxygen-deficient ZnO nanorod arrays and their enhanced field emission. *Materials Science in Semiconductor Processing, 67*, 55-61. doi:https://doi.org/10.1016/j.mssp.2017.05.012

Tacconelli, E., Carrara, E., Savoldi, A., Harbarth, S., Mendelson, M., Monnet, D. L., . . . Magrini, N. (2018). Discovery, research, and development of new antibiotics: the WHO priority list of antibiotic-resistant bacteria and tuberculosis. *Lancet Infect Dis, 18*(3), 318-327. doi:10.1016/s1473-3099(17)30753-3

Tiwari, V., Mishra, N., Gadani, K., Solanki, P. S., Shah, N. A., & Tiwari, M. (2018). Mechanism of Anti-bacterial Activity of Zinc Oxide Nanoparticle Against Carbapenem-Resistant Acinetobacter baumannii. *Front Microbiol, 9*, 1218. doi:10.3389/fmicb.2018.01218

V, L. P., & Vijayaraghavan, R. (2017). Chemical manipulation of oxygen vacancy and antibacterial activity in ZnO. *Materials Science and Engineering: C, 77*, 1027-1034. doi:https://doi.org/10.1016/j.msec.2017.03.280

Wang, J., Wang, Z., Huang, B., Ma, Y., Liu, Y., Qin, X., . . . Dai, Y. (2012). Oxygen Vacancy Induced Band-Gap Narrowing and Enhanced Visible Light Photocatalytic Activity of ZnO. *ACS Applied Materials & Interfaces, 4*(8), 4024-4030. doi:10.1021/am300835p

Xia, T., Wallenmeyer, P., Anderson, A., Murowchick, J., Liu, L., & Chen, X. (2014). Hydrogenated black ZnO nanoparticles with enhanced photocatalytic performance. *RSC Advances, 4*(78), 41654-41658. doi:10.1039/C4RA04826A

Xing, G., Wang, D., Yi, J., Yang, L., Gao, M., He, M., . . . Wu, T. (2010). Correlated d ferromagnetism and photoluminescence in undoped ZnO nanowires. *Applied Physics Letters, 96*(11), 112511. doi:10.1063/1.3340930

Xu, F. F., & Imlay, J. A. (2012). Silver(I), mercury(II), cadmium(II), and zinc(II) target exposed enzymic iron-sulfur clusters when they toxify Escherichia coli. *Appl Environ Microbiol, 78*(10), 3614-3621. doi:10.1128/aem.07368-11

Xu, X., Chen, D., Yi, Z., Jiang, M., Wang, L., Zhou, Z., . . . Hui, D. (2013). Antimicrobial Mechanism Based on H2O2 Generation at Oxygen Vacancies in ZnO Crystals. *Langmuir, 29*(18), 5573-5580. doi:10.1021/la400378t

Vita

Alexander Jacob Caron was born September 7th, 2000, in Lake Forest, Illinois. He is the son of Jennifer and Scott Caron. A 2019 graduate of Spring Hill High School in Longview, Texas, he received a Bachelor of Science degree with a major in Biology from Texas Christian University, Fort Worth, in December 2022.

In January 2023, he continues his education by enrolling in graduate study at Texas Christian University, where he received his Master of Science degree in 2024. While working on his Master in Biology, he held a Teaching Assistantship and was a member of the American Society of Microbiologist. After receiving his masters, Alexander will be pursuing this PhD of Molecular Microbiology from the University of Texas Southwestern Medical Center

ZINC OXIDE NANOPARTICLES MEDIATE BACTERIAL TOXICITY IN MUELLER-HINTON BROTH VIA Zn^{2+}

by Alexander J. Caron, Masters of Science, 2024
Department of Biology
Texas Christian University

Shauna McGillivray, Assistant Professor

Zinc oxide nanoparticles (ZnO NPs) are promising antimicrobial agents due to their broad-spectrum antibacterial activity and low production cost. Despite many studies demonstrating the effectiveness of ZnO NPs, the antibacterial mechanism is still unknown. Previous work has implicated the role of reactive oxygen species, physical damage of the cell envelope, and/or release of toxic Zn^{2+} ions as possible mechanisms of action. Assays utilizing *S. aureus* mutant strains Δ*katA* and Δ*mprF* demonstrated that hydrogen peroxide and electrostatic interactions are not crucial for mediating ZnO NP toxicity. Instead, we find Zn^{2+} accumulation mediates toxicity independent of physical contact. Through this, we conclude that soluble Zn^{2+} is the primary mechanism by which ZnO NPs mediate toxicity in Mueller-Hinton Broth. Future work investigating the effect of ZnO NP synthesis methods on Zn^{2+} dissolution could allow for the synthesis of ZnO NPs that possess chemical and morphological properties best suited for antibacterial efficacy.